nature chemistry

SUPPLEMENTARY INFORMATION

https://doi.org/10.1038/s41557-019-0297-7

In the format provided by the authors and unedited.

Ultra-fast intramolecular singlet fission to persistent multiexcitons by molecular design

Andrew B. Pun[1,9], Amir Asadpoordarvish[2,9], Elango Kumarasamy[1], Murad J. Y. Tayebjee[3,4], Daniel Niesner[1,5], Dane R. McCamey[2], Samuel N. Sanders[1,6,9]*, Luis M. Campos[1]* and Matthew Y. Sfeir[5,7,8]*

[1]Department of Chemistry, Columbia University, NewYork, NY, USA. [2]ARC Centre of Excellence in Exciton Science, School of Physics, University of New South Wales, Sydney, New South Wales, Australia. [3]Cavendish Laboratory, University of Cambridge, Cambridge, UK. [4]School of Photovoltaic and Renewable Energy Engineering, University of New South Wales, Sydney, New South Wales, Australia. [5]Center for Functional Nanomaterials, Brookhaven National Laboratory, Upton, MA, USA. [6]Rowland Institute at Harvard, Cambridge, MA, USA. [7]Photonics Initiative, Advanced Science Research Center, City University of New York, New York, NY, USA. [8]Department of Physics, Graduate Center, City University of New York, New York, NY, USA. [9]These authors contributed equally: Andrew B. Pun, Amir Asadpoordarvish, Samuel N. Sanders. *e-mail: sanders@rowland.harvard.edu; lcampos@columbia.edu; msfeir@gc.cuny.edu

Supplementary Materials

Ultrafast Intramolecular Singlet Fission to Persistent Multiexcitons by Molecular Design

Andrew B. Pun[†,1], Amir Asadpoordarvish[†,2], Elango Kumarasamy[1], Murad J.Y. Tayebjee[2,3], Daniel Niesner[1,4], Dane R. McCamey[2], Samuel N. Sanders,[†,1,5]* Luis M. Campos,[1]* Matthew Y. Sfeir[4,6,7]*

[1]Department of Chemistry, Columbia University, New York, New York 10027, United States
[2]School of Photovoltaic and Renewable Energy Engineering and // ARC Centre of Excellence in Exciton Science, School of Physics, University of New South Wales, Sydney, New South Wales 2052, Australia
[3]Cavendish Laboratory, University of Cambridge, J. J. Thomson Avenue, Cambridge CB3 0HE, United Kingdom
[4]Center for Functional Nanomaterials, Brookhaven National Laboratory, Upton, New York 11973, United States
[5]Rowland Institute at Harvard, Cambridge, MA 02142, United States
[6]Photonics Initiative, Advanced Science Research Center, City University of New York, New York, New York 10031, United States
[7]Department of Physics, Graduate Center, City University of New York, New York, New York 10016, United States

TABLE OF CONTENTS

1. Materials and Methods

General Methods: All commercially obtained reagents/solvents were used as received; chemicals were purchased from Alfa Aesar®, Sigma-Aldrich®, Acros organics®, TCI America®, Mallinckrodt®, and Oakwood® Products, and were used as received without further purification. Unless stated otherwise, reactions were conducted in oven-dried glassware under argon atmosphere. Bromo-TIPS-Tetracene **1**, BisBpin-NODIPS-Pentacene **2**, Bpin-NODIPS-Pentacene **3**, Bpin-TIPS-Pentacene **4**, Dibromo-TIPS-Tetracene **7, PT**, Dibromo-NODIPS-tetracene , and **P-Br** were synthesized according to literature procedure.(*1–5*) ^{1}H-NMR and ^{13}C-NMR spectra were recorded on Bruker 400 MHz (100 MHz for ^{13}C) and on 500 MHz (125 MHz for ^{13}C) spectrometers. Data from the ^{1}H-NMR and ^{13}C spectroscopy are reported as chemical shift (δ ppm) with the corresponding integration values. Coupling constants (*J*) are reported in hertz (Hz). Standard abbreviations indicating multiplicity were used as follows: s (singlet), b (broad), d (doublet), t (triplet), q (quartet), m (multiplet) and virt (virtual).

The mass spectral data for the compounds were obtained from XEVO G2-XS Waters® equipped with a QTOF detector with multiple inlet and ionization capabilities including electrospray ionization (ESI), atmospheric pressure chemical ionization (APCI), and atmospheric solids analysis probe (ASAP). The base peaks were usually obtained as $[M]^{+}$ or $[M+H]^{+}$ ions.

Absorption spectra were obtained on a Shimadzu UV 1800 UV-Vis spectrophotometer.

Anhydrous solvents were obtained from a Schlenk manifold with purification columns packed with activated alumina and supported copper catalyst (Glass Contour, Irvine, CA). All reactions were carried out under argon unless otherwise noted.

Details of the transient absorption experiments have been described previously.[1] Briefly, a 1 kHz amplified Ti:Sapphire system with an optical parametric amplifier is generates resonant pump pulses of ~ 100 fs. This laser is also used to generate a femtosecond supercontinuum probe in a thin sapphire plate, where delay is controlled mechanically with respect to the pump pulse. A nanosecond supercontinuum probe pulse is generated in a fiber laser (Leukos) and employed using an electronically

delayed configuration to investigate longer delayed times. The pump pulse is the same for both probe measurements. The measurements are conducted at concentrations below 100 μM, and typically ~50 μM unless otherwise noted.

Pulsed laser, continuous microwave and pulsed laser, pulsed microwave measurements were carried out using the method described in our previous report.[2] Briefly, compounds were dissolved in toluene and transferred to a sealed quartz ESR tube under nitrogen. UV-visible absorption spectroscopy was employed to ensure that no aggregation occurred. PTnP films were fabricated by firstly drop-casting N_2-degassed toluene wet-films (Sigma Aldrich, 244511-100ML) on microscope cover-glass slides (H. B. Selby, thickness: 0.2 mm). Afterward, the PTnP powders were added to the toluene wet-films to dissolve and form PTnP/toluene wet-films. The PTnP/toluene wet-films were semi-dried under a N_2-filled glove box ([O_2], [H_2O] < 1 ppm) at room temperature. The PTnP semi-dried films were transferred to 4 mm thin wall quartz ESR sample tubes (Wilmad-LabGlass, 707-SQ-100M) and the ESR sample tubes were placed in a 1 x 10^{-7} mBar vacuum environment to ensure the films are fully dried. Finally, the ESR sample tubes were sealed by a UV-curable single-component epoxy adhesive (Ossila, E132) in a N_2-filled glove box ([O_2], [H_2O] < 1 ppm).

Experiments were undertaken using a Bruker Elexsys E580. Samples were transferred to a cryogenically cooled (Oxford Instruments, CF935) resonator (Bruker, MD5) attached to an X-band microwave source (Bruker, Super X FT-ESR Bridge). A ~7 ns 599 nm or 660 nm laser pulse was used to excite the sample (Opotek, OPOLETTE). In nutation frequency measurements, the nutation pulse was applied 1.0 μs after the laser pulse at 340 mT (9.7047 GHz) and 325 mT (9.7062 GHz), respectively. The data from pulsed laser, pulsed microwave measurements was fit with a damped sine wave to establish the nutation frequency of a given transition.

2. UV-Visible Absorption Spectra

UV-visible absorption spectra were obtained as dilute solutions in toluene for all new compounds investigated in this report (Supplementary Figure 1). Notably, the materials all feature clear absorption features for pentacene, with an onset of vibronic progression near 660 nm, and features for tetracene, with an onset of absorption near 550 nm. The coupling at the 2 position of these acenes also results in a new absorption peak near 470 nm, as reported previously. The data have been normalized at the pentacene associated absorption near 660 nm to facilitate comparison. This normalization reveals that PTP features a relatively larger magnitude pentacene absorption than tetracene relative to PT2P. We ascribe this reduction in peak height the larger number of regioisomers in PT2P, resulting in peak broadening increasing the area but reducing the height of the tetracene peak. PT3P has a larger magnitude and broader tetracene feature, as it has even more regioisomers, and also more tetracenes for each pentacene. Finally, TPT features a similar number of regioisomers to PTP, and therefore has a tetracene feature that is relatively sharp, but with a significantly larger tetracene absorption relative to pentacene, as expected.

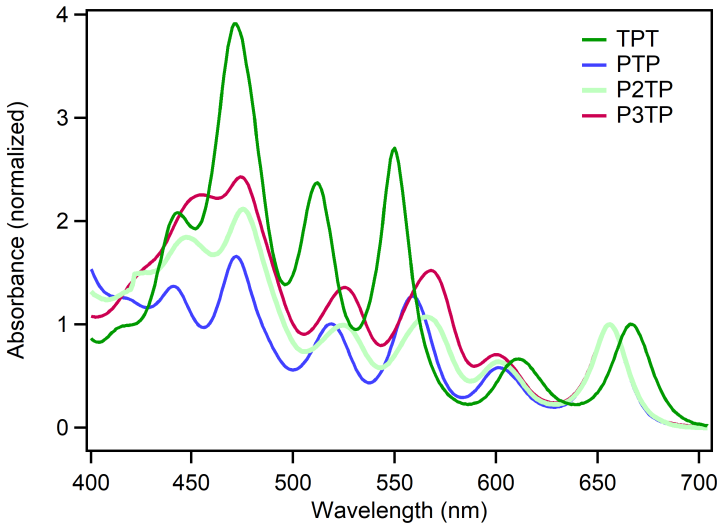

Supplementary Figure 1. UV-Visible absorption spectra of PTP, PT2P, PT3P and TPT, the new molecules reported here, as dilute (<100 μM) solutions in toluene.

3. Global Analysis

Global analysis was crucial for accurate assignment of distinct species and their respective lifetimes in transient absorption spectroscopy experiments, and was performed using the Glotaran software package.[3] This technique reproduces a dataset as a series of unique spectra with associated lifetimes. Because it treats the data set in aggregate, it provides especially accurate time constants, and because it creates a reproduced model of the data, we can compare the raw data to our model to ensure we have accurately captured the dynamics and spectra of the system. Below, we show examples of our fitting for PT3P, a representative compound discussed in this paper. In Supplementary Figure 2, we show the three species isolated from fitting the fs TA data exciting at 600 nm in toluene for PT3P. Interestingly, the splitting of the pentacene-tetracene to pentacene-pentacene triplet pair slightly more than doubles the value of the pentacene photoinduced absorption peak near 520 nm. We would expect this signal to roughly double going from one pentacene triplet to two, but this triplet pair splitting process also involves loss of tetracene associated ground state bleach in this region, resulting in an even larger signal increase.

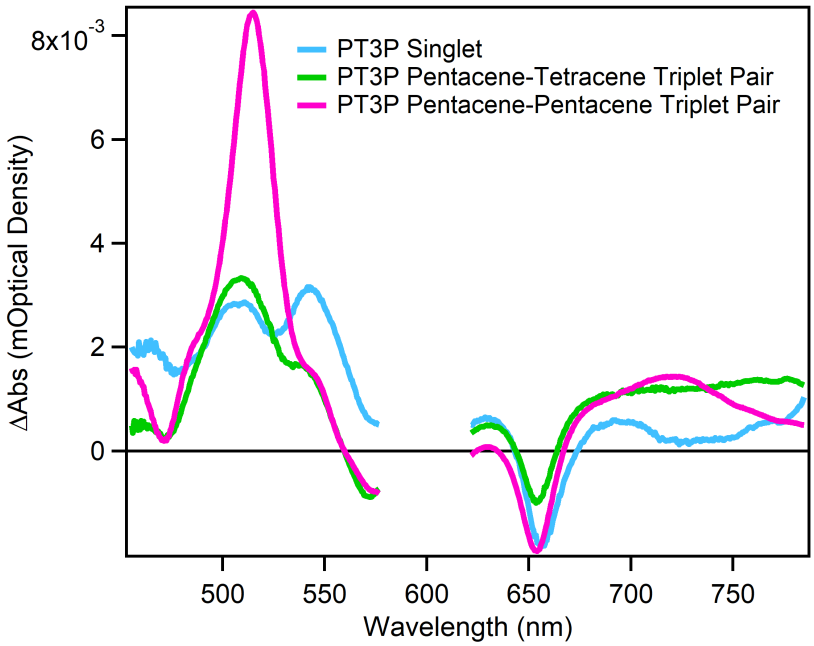

Supplementary Figure 2. Spectra isolated by global analysis of the femtosecond transient absorption spectroscopy for the singlet exciton, the pentacene-tetracene triplet pair and the final pentacene-pentacene triplet pair state

In Supplementary Figure 3, we compare kinetics at 560 nm in the raw data to fits. The global fitting agrees well with the data, and shows the decay of the singlet associated signal in this region is completed for PT3P around 2 ps. We also show the kinetics at 730 nm, where there is minimal singlet photoinduced absorption (Supplementary Figure 2). In this region, we can see a fast rise, also completed around 2 ps corresponding to singlet fission, but a secondary, slower rise as well corresponding to the rise of the second pentacene triplet as the triplet pair splitting occurs to populate the final pentacene-pentacene triplet pair state.

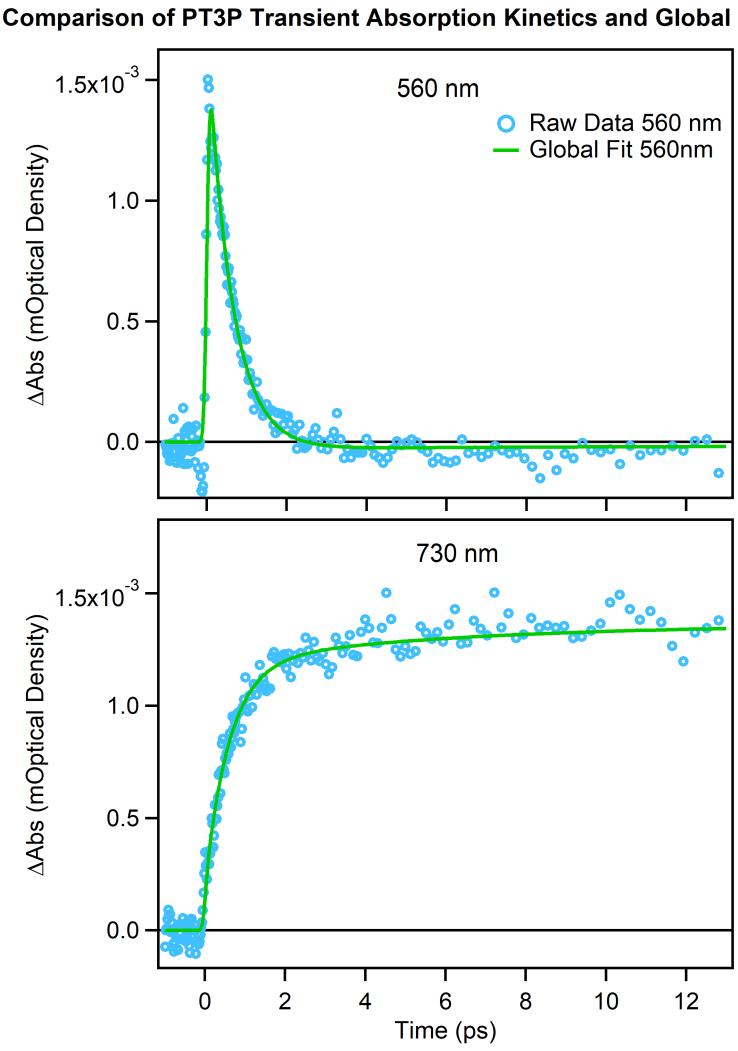

Supplementary Figure 3. Comparison of global analysis fits to raw data at 560 nm, where only singlet exciton has significant photoinduced absorption, and at 730 nm, where photoinduced absorption is dominated by triplet signal.

In Supplementary Figure 4, we compare spectra from raw data to those obtained by global fitting. The green trace shows a near-zero residual throughout, indicating a good fit for the data at times corresponding mostly to singlet (180fs), pentacene-tetracene triplet pair (1.5 ps), and the pentacene-pentacene triplet pair (25 ps).

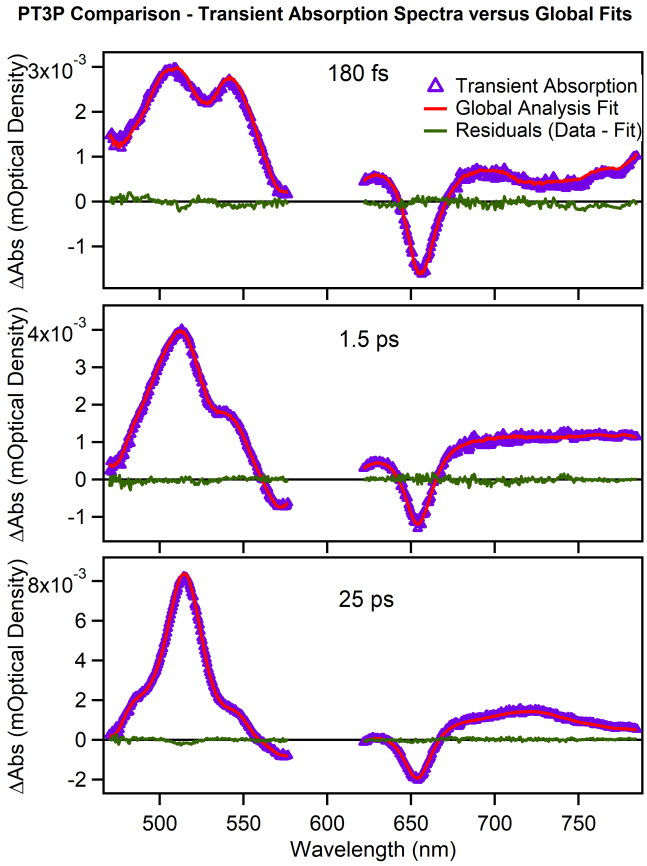

Supplementary Figure 4. Spectral comparison of raw data and global fitting at time scales dominated by singlet (180 fs), pentacene-tetracene triplet (1.5 ps), and pentacene-pentacene triplet (25 ps), as well as residuals (green).

In Supplementary Figure 5, we compile the isolated spectra from global analysis for TPT, PTP, PT2P and PT3P, all of the new compounds reported here.

In every case, the singlet exciton lineshapes are reasonably similar, with differences primarily defined by differences in ground state bleach signal among the different compounds. The singlet exciton decays in all cases concurrent with rise of a new state. For TPT, PT2P and PT3P, this new state is the pentacene-tetracene triplet pair state. In PTP, that state is not resolved. In the case of TPT, this state represents the final state,

as there is no energy cleft built in to separate this pentacene-tetracene triplet pair. In the case of PT2P and PT3P, we see this pentacene-tetracene triplet pair state decay and the rise of a third state, the pentacene-pentacene triplet pair state, seen as an increase in pentacene ground state bleach and an approximate doubling of the pentacene triplet signal with a maximum around 520 nm. In PTP, we do not resolve the intermediate, so this pentacene-pentacene triplet pair lineshape evolves directly from the singlet isolated spectrum.

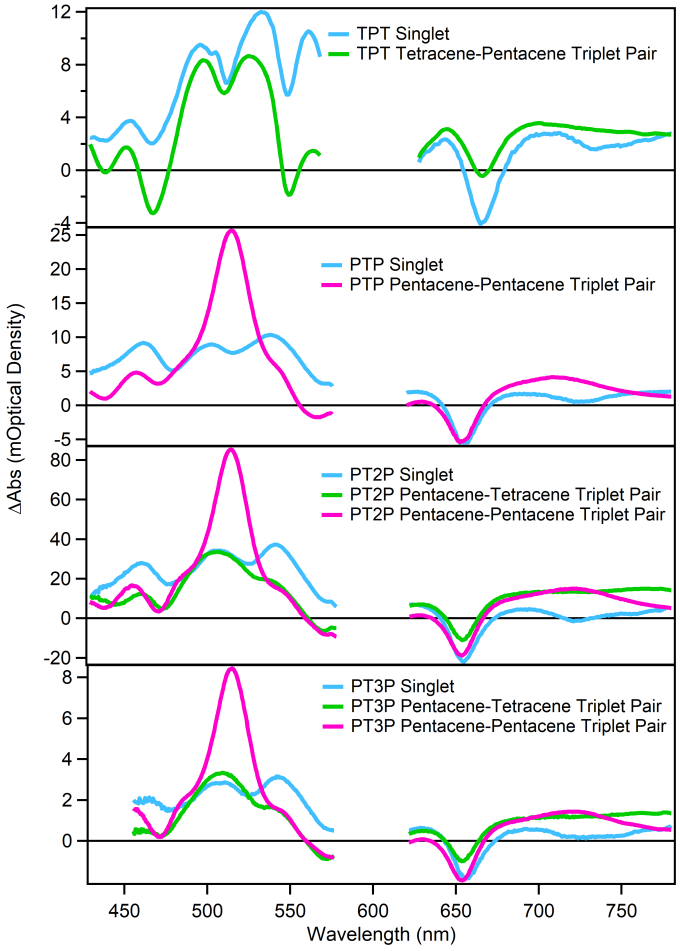

Supplementary Figure 5. Global analysis isolated spectra for all new compounds reported here, measured as dilute solutions in toluene with excitation at 600 nm

4. Singlet Fission Yield Determination

The normal triplet yield determination using triplet sensitization methods must be modified slightly to account for the heterogeneous nature of the compounds studied here. We determine all yields to be quantitative, i.e., > 199%. Detailed analysis is shown here for PT3P, but similar results were obtained for all compounds.

First, we determine the relationship between singlet exciton concentration and the magnitude of the ground state bleach signal observed in transient optical experiments. In our procedure, we avoid two potentially problematic assumptions. First, we do not simply assume that the molar extinction coefficient measured in linear measurements can be directly mapped onto the transient optical experiments. Second, we have avoided the assumption that 100% of the population of triplets from the sensitizer is transferred to the pentacene sub-ensemble since tetracene chromophores are also energetically accessible. The GSB near 660 nm is specific for pentacene occupation and the triplet-triplet absorption peak at 520 nm is dominated by pentacene. So even in an ensemble with mixed occupation, we have specific optical markers that can be used to isolate the pentacene contribution.

To determine the molar extinction coefficient associated with the ground state bleach signal, we measure the attenuated power by a PT3P solution in toluene from a stabilized 600 nm pump beam. The spot size is determined to be 0.94 mm using a CCD based beam profiler, giving a total incident fluence of 1.76×10^{14} photons/cm^2 for our experiment. To verify this method, solutions of TIPS-pentacene (TPc) and a bridged bipentacene (BP2) with known molar extinction coefficients are measured for comparison.[4]

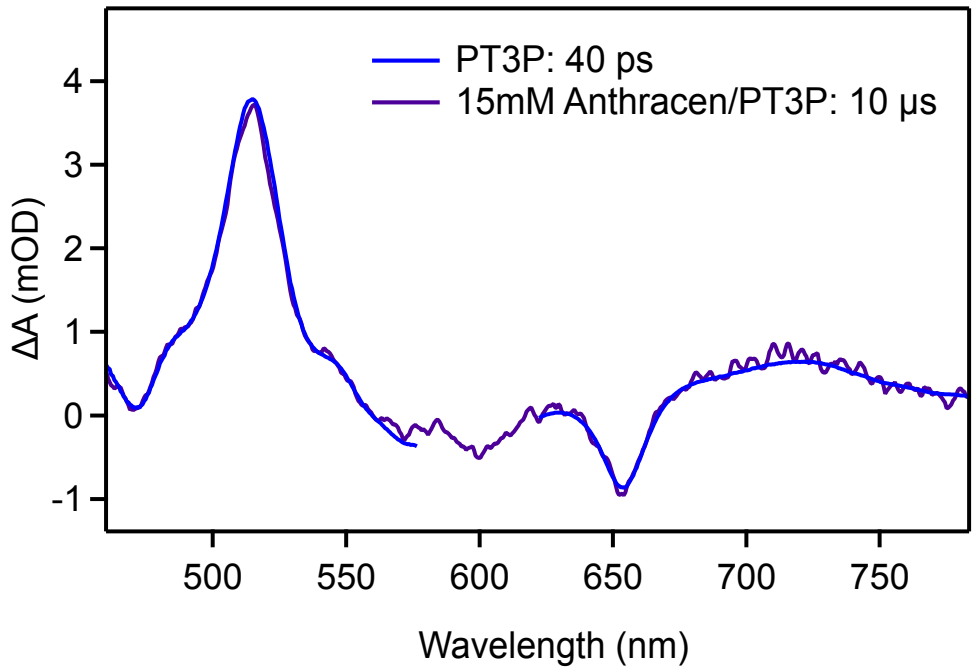

Supplementary Figure 6. Global analysis isolated spectra for all new compounds reported here, measured as dilute solutions in toluene with excitation at 600 nm

The absorbed fluence is calculated using the linear optical density at 600 nm solutions of TPc, BP2, and PT3P and is defined as (incident fluence)*(1 – 10^{-OD}).

We determine the GSB amplitude from fitting transient spectra at a fixed time (40 ps) using a linear background to account for overlapping excited state absorptions. Using the relation that one absorbed photon yields one exciton, we calculate the molar extinction coefficient for the GSB signal using the equation:

$\varepsilon_{GSB} = OD_{GSB} / (\text{Absorbed Fluence}) * 10^{-3} * N_A$

	OD @ 600 nm	Absorbed Fluence [cm^{-2}]	GSB Amplitude	ε_{GSB} [M^{-1} cm^{-1}]
TPc	0.165	5.56×10^{13}	2.3×10^{-3}	24900
BP2	0.136	4.73×10^{13}	3.3×10^{-3}	42000
PT3P	0.043	1.66×10^{13}	1.1×10^{-3}	31200

To determine the molar extinction coefficient associated with the triplet-triplet excited state absorption, we use triplet sensitization measurements. We analyze the transient spectra near the peak of the triplet population (~ 10 μs) and analyze only the signals that can be uniquely identified with occupation on the pentacene chromophores. Again, we avoid assuming that all the triplet population generated by the sensitizer is transferred to the pentacene chromophores. This also allows us to scale the sensitization spectra to match the amplitudes of the SF spectra.

Using the fitting procedure described above to extract the GSB amplitude and directly reading off the magnitude of the transient signal at 515 nm, we can determine the molar extinction coefficient associated with the triplet-triplet excited state absorption:

$\varepsilon_{triplet} = (OD_{triplet} / OD_{GSB}) * \varepsilon_{GSB} = (0.0037/0.0011) * (31200/2) = 52500\ M^{-1}\ cm^{-1}$

In the above calculation, we halve the GSB extinction coefficient by a factor of 2 in response to the fact that only half the molecule is bleached after triplet sensitization, as compared to direct photoexcitation in which the entire molecule is bleached. This assumption can be validated by comparing the ratios of the triplet to GSB peaks in the graph above. As both SF and triplet sensitization yield the same peak ratios, and our other data has confirmed that SF is indeed occurring, then this assumption is valid. This factor of two is further validated by global analysis, which shows that the bleach magnitude at 660 nm is halved when the pentacene-tetracene triplet pair is transiently occupied (Supplementary Figure 5). We note that this value is nearly identical to that obtained in bipentacene compounds, further supporting our approach.

From this, we can readily calculate our singlet fission yield:

$[triplet]/[singlet] = (OD_{triplet} / OD_{GSB}) * \varepsilon_{GSB} / \varepsilon_{triplet} = (3.7/1.1)*(31200/52500) = 1.99$

5. Pump Wavelength Independence

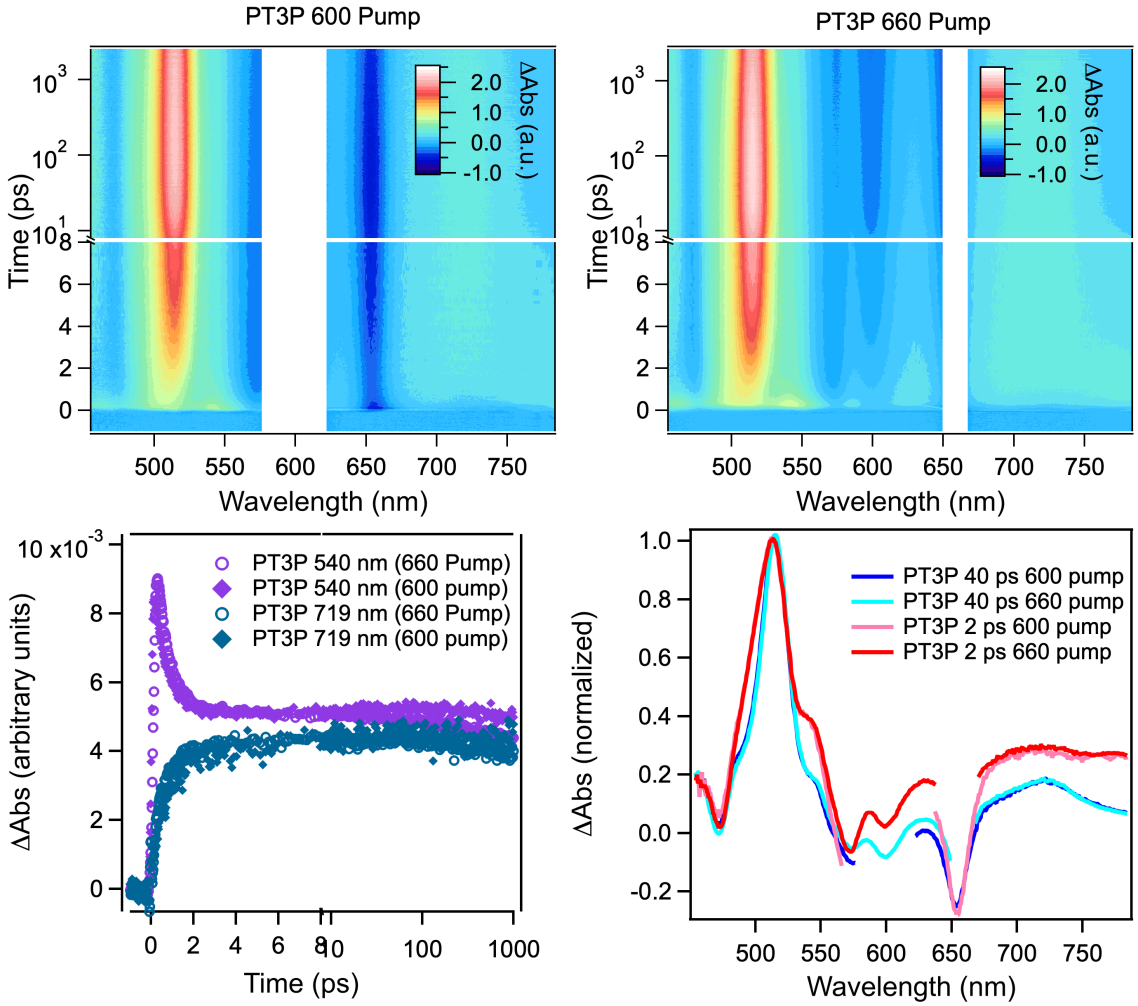

Supplementary Figure 7. Singlet fission dynamics for pumping at 600 nm and 660 nm are identical. Here, we show transient absorption measurements for **PT3P**, including (top) raw data, (bottom left) kinetic traces, and (bottom right) spectral transients.

6. NIR Transient Absorption Data

The NIR spectral region contains specific spectral markers for the correlated triplet pair that can be used to reinforce the conclusions drawn from the analysis of the visible TA data. Specifically, it has been found that a distinct NIR excited state absorption feature is a marker for strongly bound triplet pairs on contiguous chromophores, in which significant mixing of the singlet and triplet electronic manifolds occurs. This feature, which can be seen here near 1500 nm for PT2P and PT3P is present in our data, has been assigned to a transition of the triplet pair state to a high energy singlet state ($^1(T_{1[\mathbf{P}]}T_{1[\mathbf{T}]}) \rightarrow S_n$). The higher energy transition seen at earlier times is the direct $S_1 \rightarrow S_n$ transition.

The $^1(T_{1[\mathbf{P}]}T_{1[\mathbf{T}]}) \rightarrow S_n$ spectral feature appears with the singlet fission time constant and decays on the same picosecond timescales that has been assigned as the relaxation from the P-T triplet pair to the P-P triplet pair in PT2P and PT3P. As in our previous analysis, the lifetime in the pentacene-tetracene triplet pair is unresolved in PTP due to ultrafast relaxation to the pentacene triplet pair. In PT dimer and TPT, the contiguous triplet pair state persists during the entire triplet pair population lifetime.

	PT	**TPT**	**PT1P**	**PT2P**	**PT3P**
S_1	0.93 ps	0.49 ps	0.90 ps	0.51 ps	0.52 ps
$^m(T_{1[\mathbf{P}]}T_{1[\mathbf{T}]})$	2600 ps	2500 ps	not resolvable	3.0 ps	5.3 ps

Supplementary Table 1. Summary of time constants extracted from global analysis of NIR transient absorption spectra.

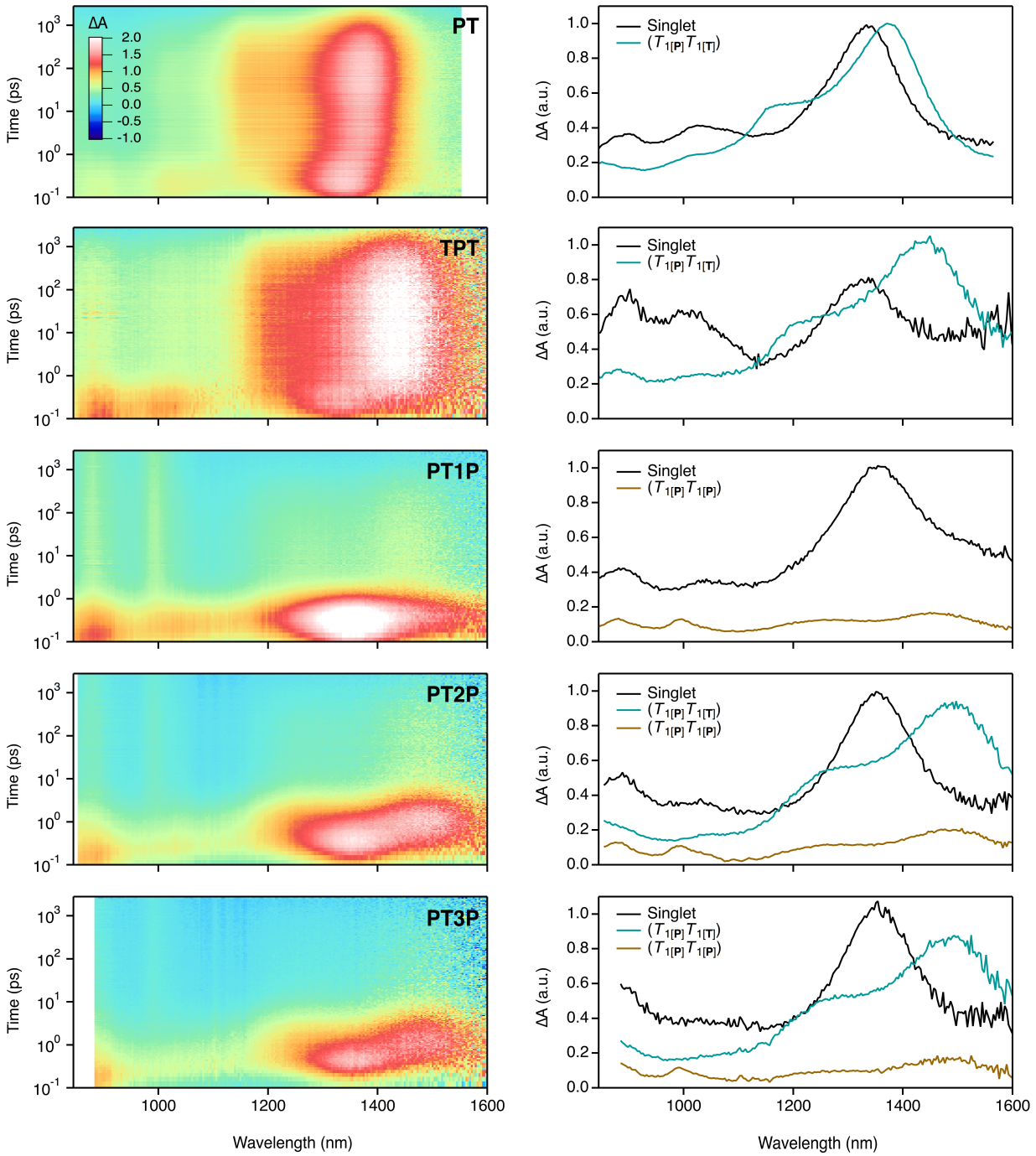

Supplementary Figure 8. NIR transient absorption spectra (left) and global analysis (right) for PT, TPT, PT1P, PT2P, and PT3P compounds.

7. Pulsed Electron Spin Resonance

In Supplementary Figure 9, we show the results of pulsed laser pulsed microwave electron spin resonance experiments for PT3P in toluene at 80K. We have described these experiments before, but briefly, we photoexcite to populate excited states, and then use pulsed microwave to nutate these states. The spin of the state affects the rate of nutation, helping to identify quintets, triplets or other species. Supplementary Figure 9a shows the echo amplitude as a function of nutation pulse length at 340 mT, while Supplementary Figure 9b shows the same data at 325 mT.

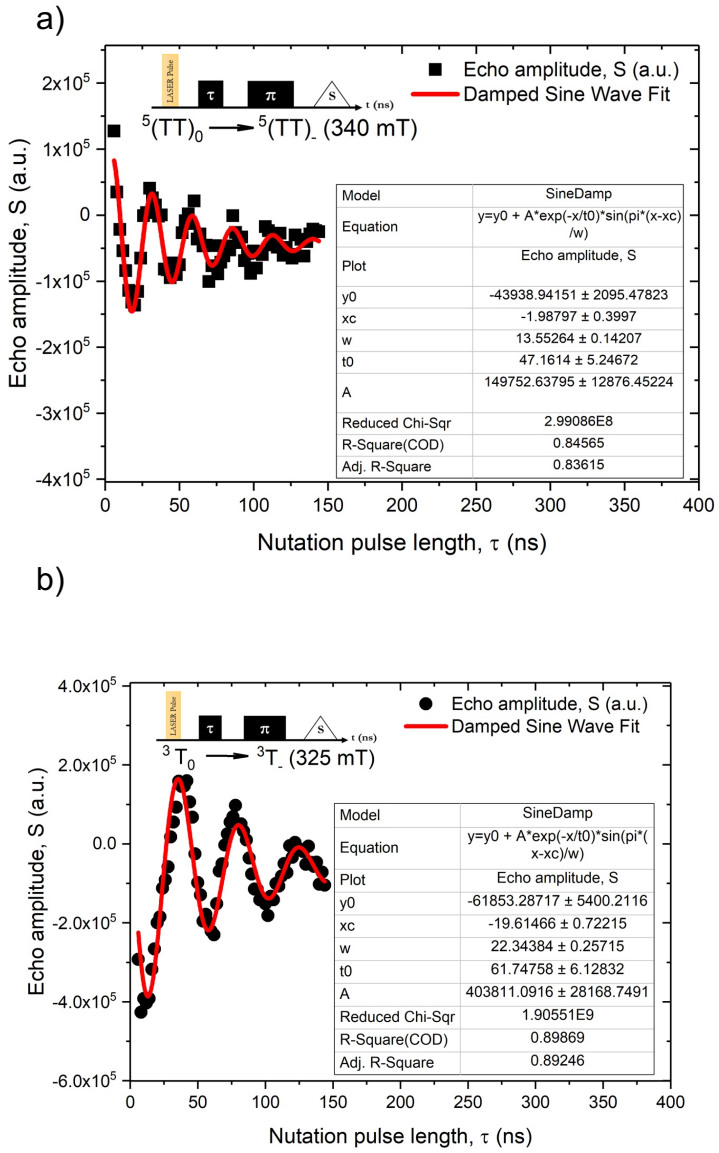

Supplementary Figure 9. Nutation data of the $^{5}(TT)_0 \leftrightarrow {}^{5}(TT)_{-1}$ (solid black squares) (a) and $^{3}T_0 \leftrightarrow {}^{3}T_{-1}$ (solid black circles) (b) at microwave frequencies of 9.7047 GHz and 9.7062 GHz and magnetic fields of 340 mT and 325 mT, respectively, 1 μs after the laser pulse illuminated a PT3P solution in toluene at 80K. The schematic inset shows the pulse sequence used, where π-pulse corresponds to a complete inversion of the spin. Solid red lines are Damped Sine Wave fits and the inset tables are showing the fitting information.

8. Thin Film Data

In general, intermolecular interactions become important in thin films and intermolecular SF can kinetically compete with intramolecular fission. However, in these particular compounds, intermolecular interactions are extremely weak in the solid state and the energy cleft design still holds.

Here, we show that the time scales extracted from transient absorption data in solution are nearly identical in the solid state, with SF time constants on the order of 500 fs for all PTnP compounds. Furthermore, only in PT2P and PT3P do we clearly resolve an intermediate state that corresponds to the strongly bound, contiguous triplet pair.

	PT1P	**PT2P**	**PT3P**
S_1	0.45 ps	0.3 ps	0.5 ps
$^{m}(T_{1[\mathbf{P}]}T_{1[\mathbf{T}]})$	not resolvable	2.8 ps	7.0 ps

Supplementary Table 2. Summary of time constants extracted from global analysis of thin films.

In addition, we have found that the recombination dynamics follow the solution phase trend, with a distinct biexponential decay dynamics featuring the 50% amplitude distribution. As is expected for an intrinsically intramolecular decay process, the recombination kinetics are independent of laser fluence.

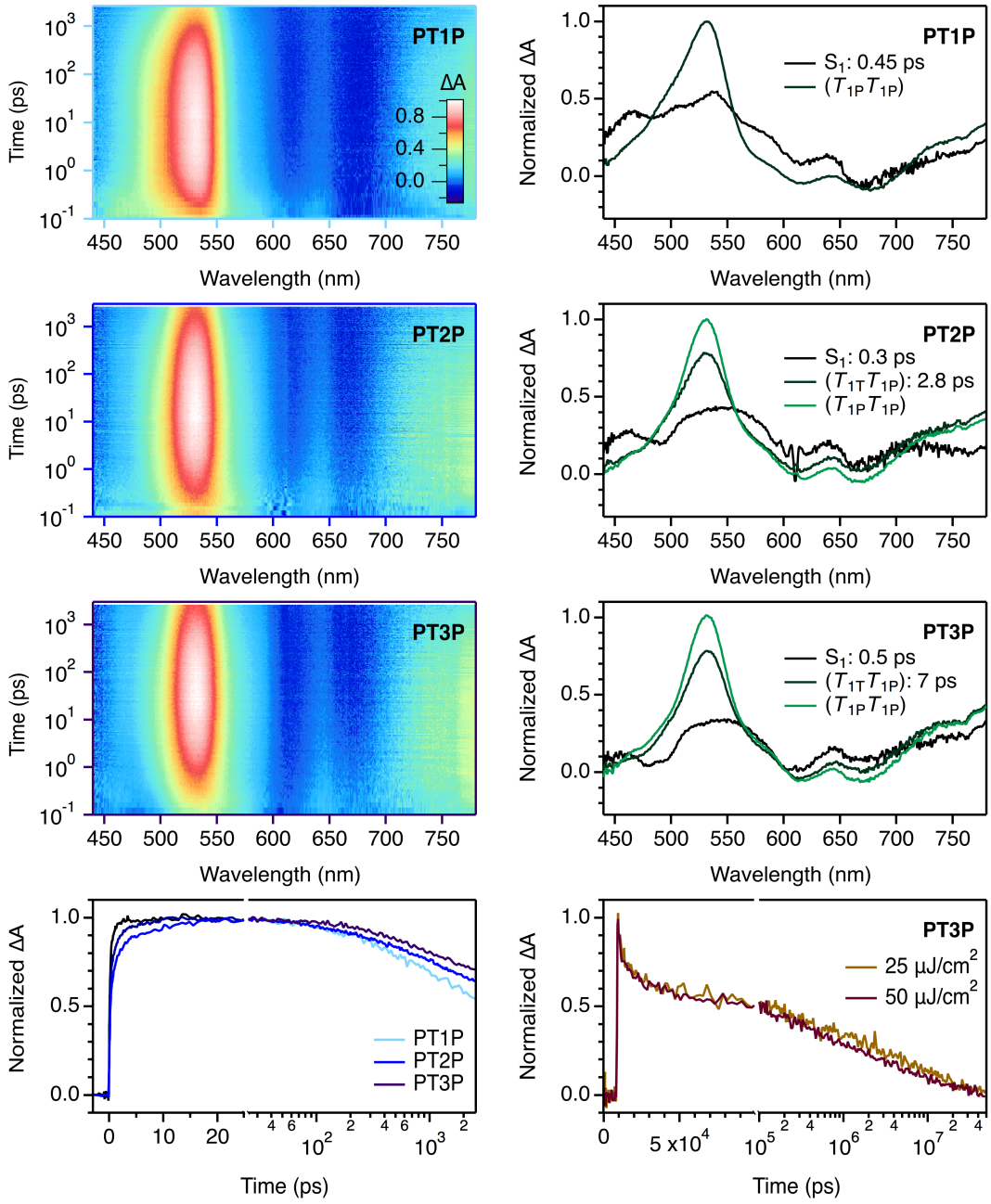

Supplementary Figure 10. The first three rows show the raw transient absorption (left) and global analysis (right) of thin films of PTnP compounds. The bottom row shows (left) a kinetic cut corresponding to the maximum of the triplet excited state absorption signal at ~ 515 nm and (right) full population dynamics exhibiting the characteristic biexponential decay and power independence of an intramolecular decay process.

In addition, time-resolved EPR measurements on thin films that clearly shows the faster rise of the free triplet signal in going from PT1P to PT3P, as was observed in solution. This effect can be alternatively seen by plotting spectral slices taken at a time after formation but before significant population decay occurs (chosen here to be ~ 1 us). Supplementary Figure 11A-C shows that the net quintet state (S=2) as well as free triplets (S=1) are forming rapidly in PTnP films analogous to PTnP compounds isolated in a frozen toluene matrix (Figure 4). In Supplementary Figure 11D-C, we compare the spectral slices of tr-ESR on PTnP aggregated films 1μs after the laser pulse. The ratio of the free triplet signal (~ 365 mT) compared to the correlated triplet signal (~ 350 mT) monotonically increases as the length of the tetracene bridge increases, reflecting the more favorable kinetics to form free triplet pairs that do not readily undergo parasitic triplet pair recombination.

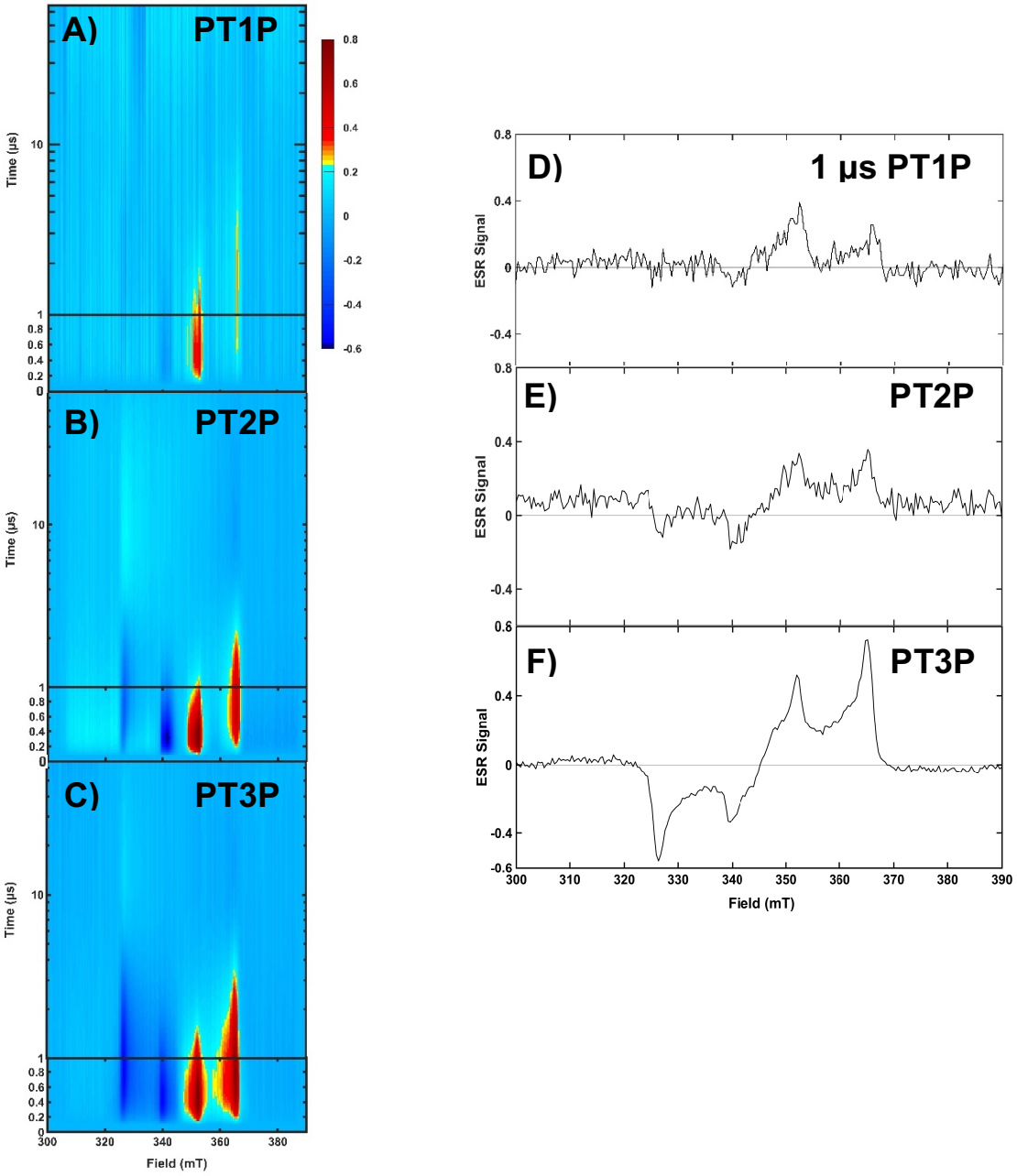

Supplementary Figure 11. Transient ESR spectral 2D maps and 1µs delayed after flash slices of (a & d) PT1P, (b & e) PT2P, and (c & f) PT3P thin films after excitation by a pulsed laser at 599 nm (3 mW). The thin-film samples were kept at 80 K in a 9.6-9.7 GHz microwave resonator.

9. Cyclic Voltammogram

Cyclic voltammetry measurements taken using a Bio-Logic VSP-300 potentiostat, using a glassy carbon working electrode, Ag wire reference electrode, and Pt wire counter electrode. Measurements were done with a scan rate of 75 mV/s in DCM with 0.1 M tetrabutylammonium hexafluorophosphate as the electrolyte after sparging with argon. All measurements were calibrated with a ferrocene/ferrocenium (Fc/Fc+) redox couple.

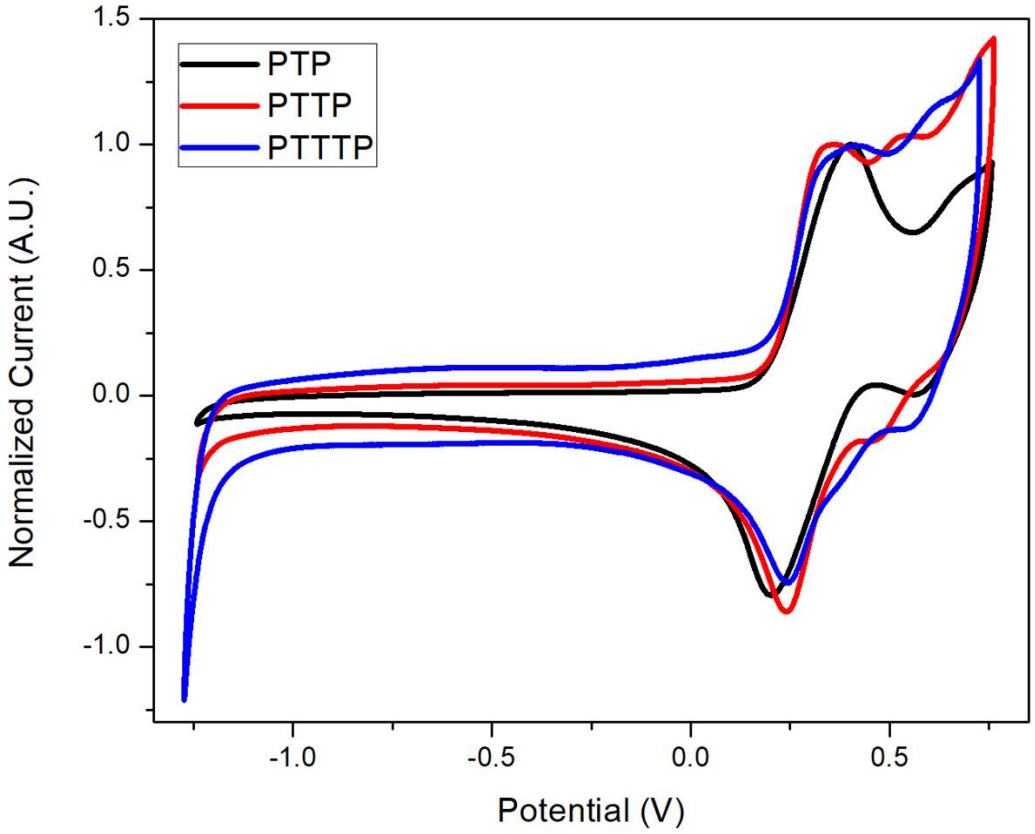

Supplementary Figure 12: Cyclic voltammograms of PTP (black), PTTP (red), and PTTTP (blue). Normalized to the first oxidation peak in the forward direction. For reference, tips pentacene has been reported in literature.[5]

10. Singlet Fission in Pentacene-Anthradithiophene-Pentacene (PADTP)

PADTP behaves similarly to **PT1P**, showing rapid singlet fission and a high free triplet yield, validating the energy cleft design for other chromophore systems.

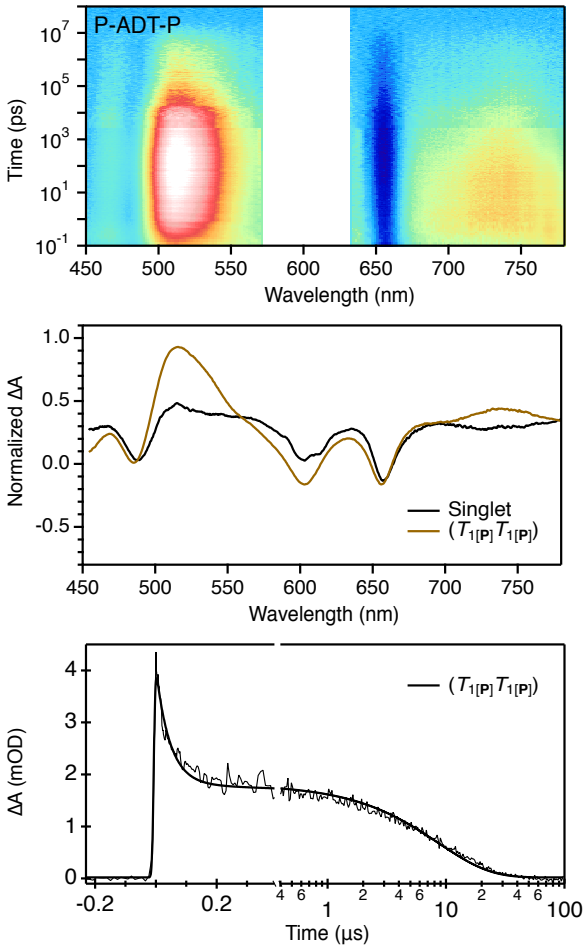

Supplementary Figure 13: (Top) Raw transient absorption data and (middle) global analysis of **PADTP** in dilute toluene solution. (Bottom) The triplet recombination dynamics are very similar to **PTP**, with a ~50 ns fast component dominating until the 45% amplitude threshold is reached, followed by decay at the one triplet lifetime.

Transient absorption measurements reveal that the excited state dynamics of **PADTP** are nearly identically to those of **PTP** (Supplementary Figure 13). **PADTP** exhibits a singlet fission time constant of ~ 700 fs and an unresolvable relaxation to a set of weakly coupled pentacene triplets. Long lived population of the ADT triplet is not observed, and ruled out by spectral analysis (Supplementary Figure 14). The transient

spectra corresponding to the ADT triplet is determined by sensitization of an ADT monomer in solution. The decay of pentacene triplets follows the expected behavior and are distinguished by their extremely long-lived triplet population and ~ 45% population sub-ensemble that decay at the mono triplet exciton lifetime. These data show that a significant reduction of the energetic offset between the intermediate and final triplet pair state is possible while maintaining the favorable triplet exciton dynamics seen in previously studied energy cleft compounds (**PTnP**). These results confirm the generality of the energy cleft design.

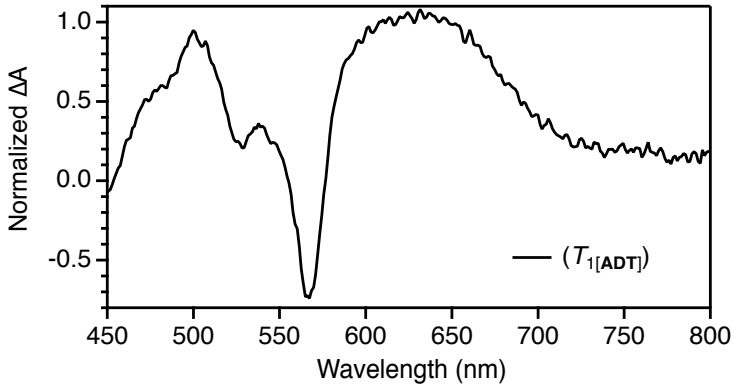

Supplementary Figure 14. Triplet sensitization of an ADT monomer in dilute toluene solution.

11. Synthesis

Throughout the synthetic procedure described below, R_1 denotes (Triisopropylsilyl)acetylene, R_2 denotes (n-octyl,diisopropylsilyl) acetylene.

Synthesis of PT-Br

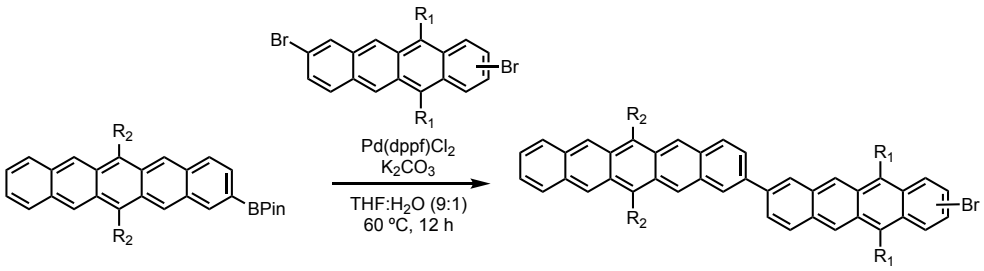

Bpin-NODIPS-Pentacene (322 mg, 0.36 mmol), Dibromo-TIPS-tetracene (797 mg, 1.07 mmol), K_2CO_3 (249 mg, 1.8 mmol) and $Pd(dppf)Cl_2$·DCM (29 mg, 0.04 mmol) were added to a reaction vial. Sequential vacuum and argon was used to degas the mixture. The solids were then dissolved in a 15 mL of a 9:1 mixture of dry THF: degassed water. The reaction was brought to 60 °C and allowed to stir for 12 h. The reaction was cooled to room temperature. The crude reaction mixture was concentrated and purified by 3% neutral alumina (3-7% $CHCl_3$ in Hexanes) to obtain **PT-Br** as a burgundy solid. (300 mg, 58% Yield).

^{1}H-NMR (400 MHz, $CDCl_3$, δ ppm): 9.39-9.32 (m, 5H), 9.24 (s, 1H), 9.10-9.09 (m, 1H), 8.82-8.79 (m, 1H), 8.39 (s, 1H), 8.22-8.21 (m, 1H), 8.14-8.09 (m, 2H), 8.03-8.00 (m, 2H), 7.98-7.92 (m, 2H), 7.56-7.53 (m, 1H), 7.47-7.44 (m, 2H), 1.84-1.78 (m, 4H), 1.46-1.35 (m, 77H), 1.30-1.25 (m, 9H), 1.18-1.15 (m, 4H), 1.03-0.99 (m, 4H), 0.87-0.83 (m, 3H) and 0.76-0.72 (m, 3H).

^{13}C-NMR (100 MHz, $CDCl_3$, δ ppm): 138.90, 138.78, 137.73, 133.37, 133.13, 132.80, 132.73, 132.51, 132.42, 132.38, 132.18, 131.64, 131.01, 130.97, 130.88, 130.70, 130.48, 130.36, 130.18, 129.65, 129.62, 129.52, 128.69, 128.33, 126.95, 126.87, 126.68, 126.40, 126.28, 126.16, 126.08, 125.57, 125.44, 120.42, 120.36, 118.95, 118.81, 118.56, 118.42, 107.78, 107.60, 106.84, 106.30, 104.57, 103.82, 103.61, 34.11, 34.02, 31.98, 31.90, 29.53, 29.47, 29.39, 25.03, 24.98, 22.68, 22.60, 19.05, 19.01, 18.77, 18.49, 14.09, 13.99, 12.24, 11.66, 10.57, 10.50.

MS (APCI+): Calculated $[M+H]^+$: 1443.7963; Observed: 1443.953.2310.

Synthesis of TPT

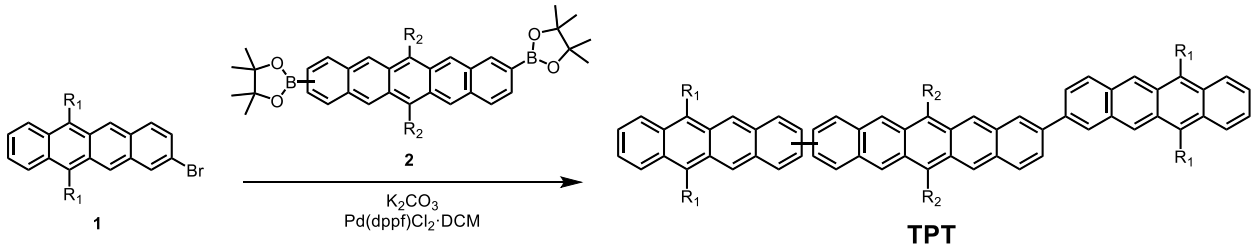

1 (70 mg, .098 mmol)**, 2** (42 mg, .045 mmol), K_2CO_3 (31 mg, 0.22 mmol) and Pd(dppf)Cl_2·DCM (3.64 mg, 0.004 mmol) were added to a reaction vial. Sequential vacuum and argon was used to degas the mixture. The solids were then dissolved in a 8 mL of a 9:1 mixture of dry THF: degassed water. The reaction was brought to 65 °C and allowed to stir overnight. The reaction was cooled to room temperature. The crude reaction mixture was concentrated and purified by chromatography on silica gel (5% DCM in Hexanes) to obtain **TPT** as a burgundy solid. (29 mg, 34% Yield).

^{1}H-NMR (400 MHz, $CDCl_3$, δ ppm): 9.43 (s, 4H), 9.36 (m, 4H), 8.66 (m, 4H), 8.38 (m, 4H), 8.18 (t, 4H), 7.99 (d, 2H), 7.95 (d, 2H), 7.57 (m, 4H), 1.82 (m, 6H), 1.45-0.6 (m, 140H).

^{13}C-NMR (125 MHz, $CDCl_3$, δ ppm): 137.94, 137.88, 137.83, 132.96, 132.85, 132.51, 131.76, 131.62, 131.29, 130.93, 130.77, 129.77, 129.65, 127.58, 127.02, 126.95, 126.91, 126.37, 126.22, 126.05, 118.89, 118.75, 106.19, 106.07, 104.12, 104.06, 34.30, 34.25, 34.20, 32.13, 32.06, 31.98, 29.74, 29.69, 29.64, 29.56, 29.54, 29.52, 25.28, 25.21, 25.15, 22.82, 22.76, 22.71, 19.16, 19.14, 18.96, 18.95, 18.93, 18.66, 18.65, 14.27, 14.18, 14.07, 12.37, 11.79, 10.67.

MS (ESI): Calculated $[M+H]^+$: 1953.2336; Observed: 1953.2310.

Synthesis of PTP

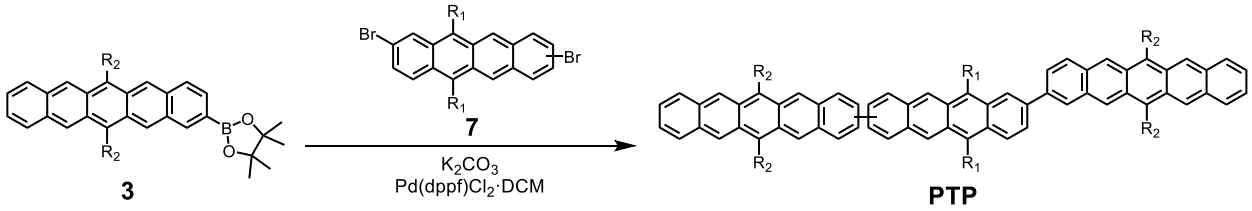

3 (60 mg, .066 mmol)**, 7** (22 mg, .03 mmol), K_2CO_3 (21 mg, .15 mmol) and Pd(dppf)Cl_2·DCM (2.5 mg, .003 mmol) were added to a reaction vial. Sequential vacuum and argon was used to degas the mixture. The solids were then dissolved in a 8 mL of a 9:1 mixture of dry THF: degassed water. The reaction was brought to 65 °C and allowed to stir overnight. The reaction was cooled to room temperature. The crude reaction mixture was concentrated and purified by chromatography on silica gel (25% DCM in Hexanes) to obtain **PTP** as a burgundy solid. (39 mg, 61% Yield).

^{1}H-NMR (400 MHz, $CDCl_3$, δ ppm): 9.45 (s, 1H), 9.39 (m, 3H), 9.33 (m, 6H), 9.11 (s, 1H), 8.82 (dd, 1H), 8.41 (s, 1H), 8.38 (d, 2H), 8.19 (dd, 2H), 8.10 (t, 2H), 7.97 (m, 7H), 7.43 (m, 4H), 1.80 (m, 8H), 1.54 (m, 8H), 1.45-0.70 (m, 150H).

Limited solubility and large number of unique carbons of material prevented the acquisition of a ^{13}C-NMR.

MS (ESI): Calculated $[M]^+$: 2143.3999; Observed: 2143.3999.

Synthesis of PT2P

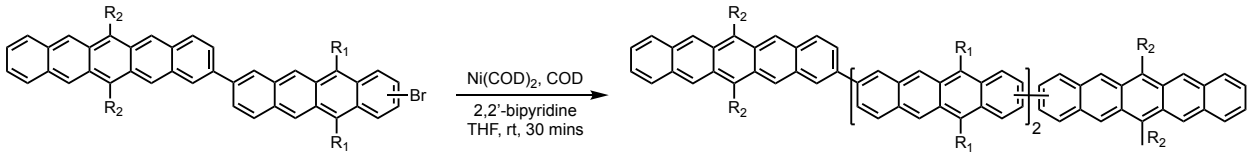

To a dry vial in a glove box, added $Ni(COD)_2$ (9.5 mg, 0.035 mmol, 1.0 equiv), COD (7.6 mg, 0.07 mmol), 2,2'-bipyridine (5.5 mg, 0.035 mmol) and THF (3 mL). The mixture immediately turned purple and to this solution added a solution of **PT-Br** (50 mg, 0.035 mmol) in THF (2 mL) slowly. The resulting solution was stirred at room temperature under dark for 30 mins. The solution was concentrated and purified on a alumina column (packed on a 20 mL syringe) using first hexanes to remove COD and 10% DCM:hexanes to elute the product as a burgundy solid. (36 mg, 45% Yield).

^{1}H-NMR (400 MHz, $CDCl_3$, δ ppm): 9.48-9.34 (m, 13H), 9.22 (s, 1H), 9.14 (m, 2H), 8.86-8.81 (m, 3H), 8.47-8.41 (3, 5H), 8.28-8.19 (m, 5H), 8.04-7.97 (m, 13H), 7.47-7.44 (m, 4H), 1.82-1.79 (m, 13H), 1.44-1.36 (m, 163H), 1.29 (m, 32H), 1.19-1.17 (m, 13H), 1.04-0.99 (m, 13H), 0.93-0.86 (m, 27H) and 0.77-0.75 (m, 9H).

Limited solubility and large number of unique carbons prevented the acquisition of a ^{13}C-NMR.

MS (MALDI+): Calculated $[M]^+$: 3457.2483; Observed: 3457.1240.

Synthesis of PT3P

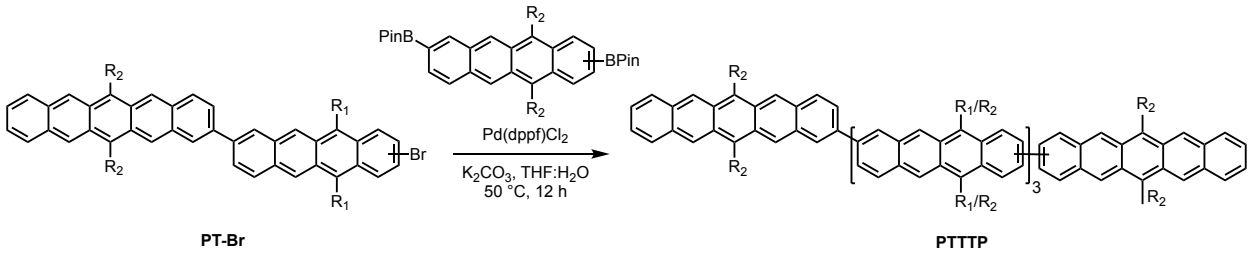

PT-Br (60 mg, 0.042 mmol, 2.2 equiv)**, Bis-Bpin NODIPS tetracene** (17 mg, 0.019 mmol, 1.0 equiv), K_2CO_3 (29 mg, 0.21 mmol) and $Pd(dppf)Cl_2 \cdot DCM$ (3.4 mg, 0.0042 mmol) were added to a reaction vial. Sequential vacuum and argon was used to degas the mixture. The solids were then dissolved in a 4 mL of a 9:1 mixture of dry THF: degassed water. The reaction was brought to 50 °C and allowed to stir overnight under dark. The reaction was cooled to room temperature. The crude reaction mixture was concentrated and purified by chromatography on silica gel (25% DCM in Hexanes) to obtain **PT3P** as a burgundy solid. (30 mg, 45% Yield).

^{1}H-NMR (400 MHz, $CDCl_3$, δ ppm): 9.39-9.32 (m, 10H), 9.24 (s, 2H), 9.09-9.09 (m, 2H), 8.82-8.79 (m, 2H), 8.39 (s, 2H), 8.22 (s, 2H), 8.14-8.09 (m, 4H), 8.04-8.01 (m, 4H), 7.97-7.92 (m, 4H), 7.56-7.54 (m, 2H), 7.47-7.44 (m, 4H), 1.82-1.79 (m, 8H), 1.42-1.36 (m, 142H), 1.28 (m, 23H), 1.18-1.15 (m, 9H), 1.03-0.99 (m, 9H), 0.87-0.84 (m, 9H) and 0.76-0.72 (m, 8H).

Limited solubility and large number of unique carbons of material prevented the acquisition of a ^{13}C-NMR.

MS (MALDI+): Calculated $[M]^+$: 2729.7447; Observed: 2730.7471.

Synthesis of Bis-Bpin ADT

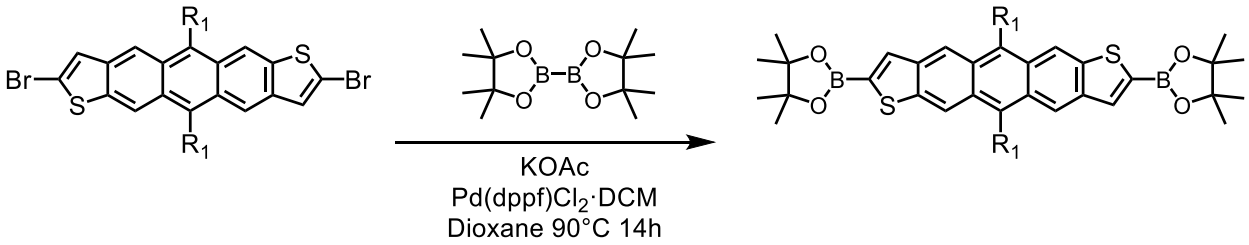

Di-Br ADT[1] (300 mg, 0.37 mmol)**,** Bis(pinacolato)diboron (282 mg, 1.11 mmol), KOAc (109 mg, 1.11 mmol) and Pd(dppf)Cl_2·DCM (30 mg, 0.037 mmol) were added to a reaction vial. Sequential vacuum and argon was used to degas the mixture. The solids were then dissolved in 4 mL of dry dioxane. The reaction was brought to 90 °C and allowed to stir overnight under dark. The reaction was cooled to room temperature. The crude reaction mixture was concentrated and purified by chromatography on silica gel to obtain **Bis-Bpin ADT** as a burgundy solid. (250 mg, 75% Yield).

^{1}H-NMR (500 MHz, $CDCl_3$, δ ppm): 9.24-9.19 (m, 4H), 8.01-7.97 (m, 2H), 1.47-1.41 (m, 24H), 1.39-1.31 (m, 42H).

^{13}C NMR (125 MHz, $CDCl_3$, δ ppm): δ 142.45, 142.13, 141.28, 141.08, 134.58, 130.73, 130.40, 130.29, 129.95, 122.77, 119.99, 118.12, 106.36, 104.28, 84.97, 84.95, 25.01, 19.13, 19.09, 11.76.

MS (ESI+): Calculated $[M]^+$: 902.4614; Observed: 902.4621.

Synthesis of PADTP

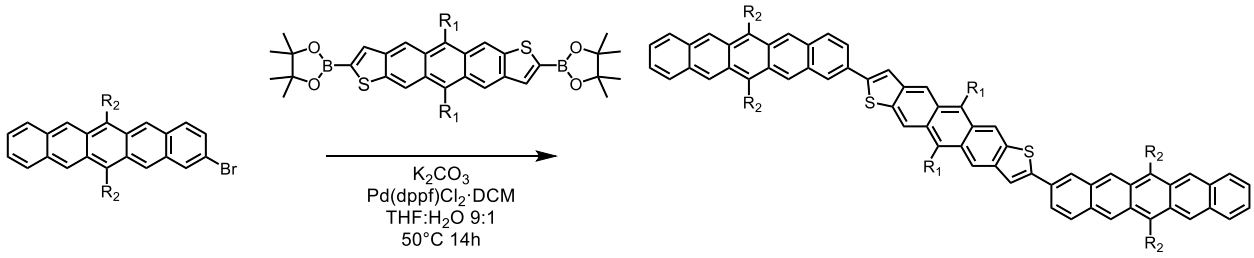

P-Br (112 mg, 0.13 mmol)**, Bis-Bpin ADT** (50 mg, 0.06 mmol), K_2CO_3 (39 mg, 0.3 mmol) and Pd(dppf)Cl_2·DCM (4.6 mg, 0.006 mmol) were added to a reaction vial. Sequential vacuum and argon was used to degas the mixture. The solids were then dissolved in a 4 mL of a 9:1 mixture of dry THF: degassed water. The reaction was brought to 50 °C and allowed to stir overnight under dark. The reaction was cooled to room temperature. The crude reaction mixture was concentrated and purified by chromatography on alumina to obtain **PADTP** as a black solid. (34 mg, 28% Yield).

^{1}H-NMR (400 MHz, $CDCl_3$, δ ppm): 9.40-8.87 (m, 12H), 8.14- 7.82 (m, 8H), 7.80-7.66 (m, 2H), 7.61-7.27 (m, 5H), 7.25-7.13 (m, 1H), 1.85-1.76 (m 6H), 1.58-1.53 (m, 6H), 1.49-1.14 (m, 130H), 1.09-0.94 (m, 12H), 0.87-0.81 (m, 6H), 0.78-0.72 (m, 6H).

Limited solubility and large number of unique carbons prevented the acquisition of a ^{13}C-NMR.

MS (MALDI+): Calculated $[M]^+$: 2205.328; Observed: 2205.408.

12. NMR Spectra

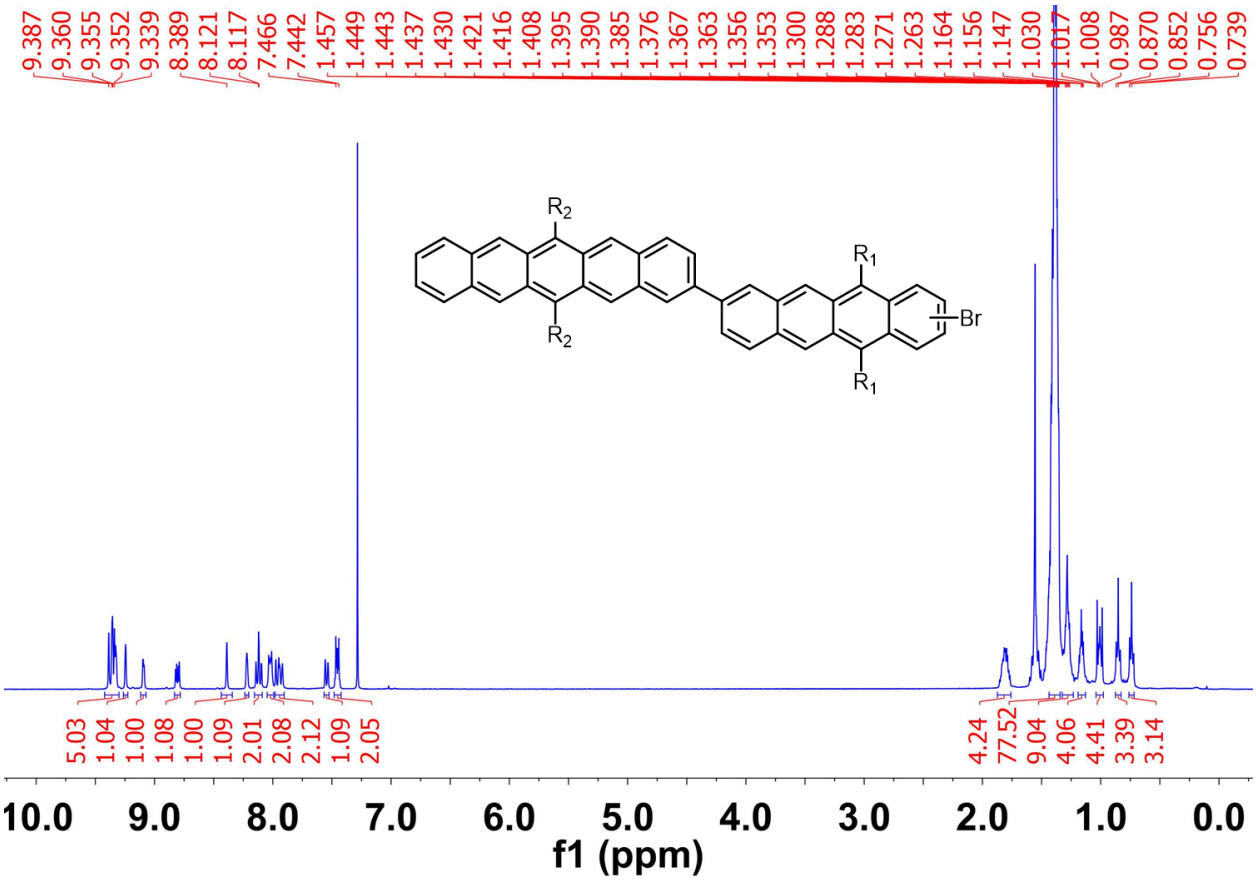

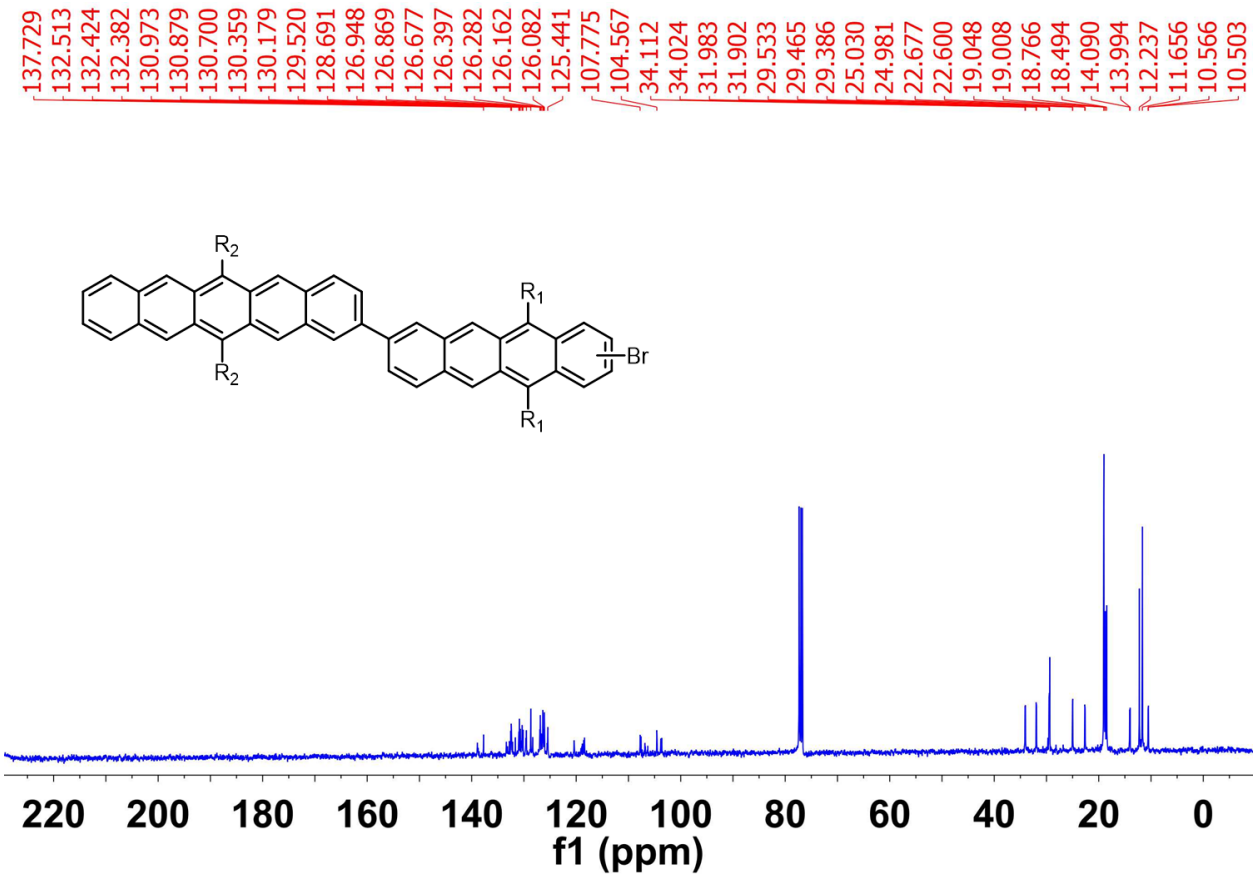
137.729
132.513
132.424
132.382
130.973
130.879
130.700
130.359
130.179
129.520
128.691
126.948
126.869
126.677
126.397
126.282
126.162
126.082
125.441
107.775
104.567
34.112
34.024
31.983
31.902
29.533
29.465
29.386
25.030
24.981
22.677
22.600
19.048
19.008
18.766
18.494
14.090
13.994
12.237
11.656
10.566
10.503
R2
R1
Br
220
200
180
160
140
120
100
80
60
40
20
0
f1 (ppm)

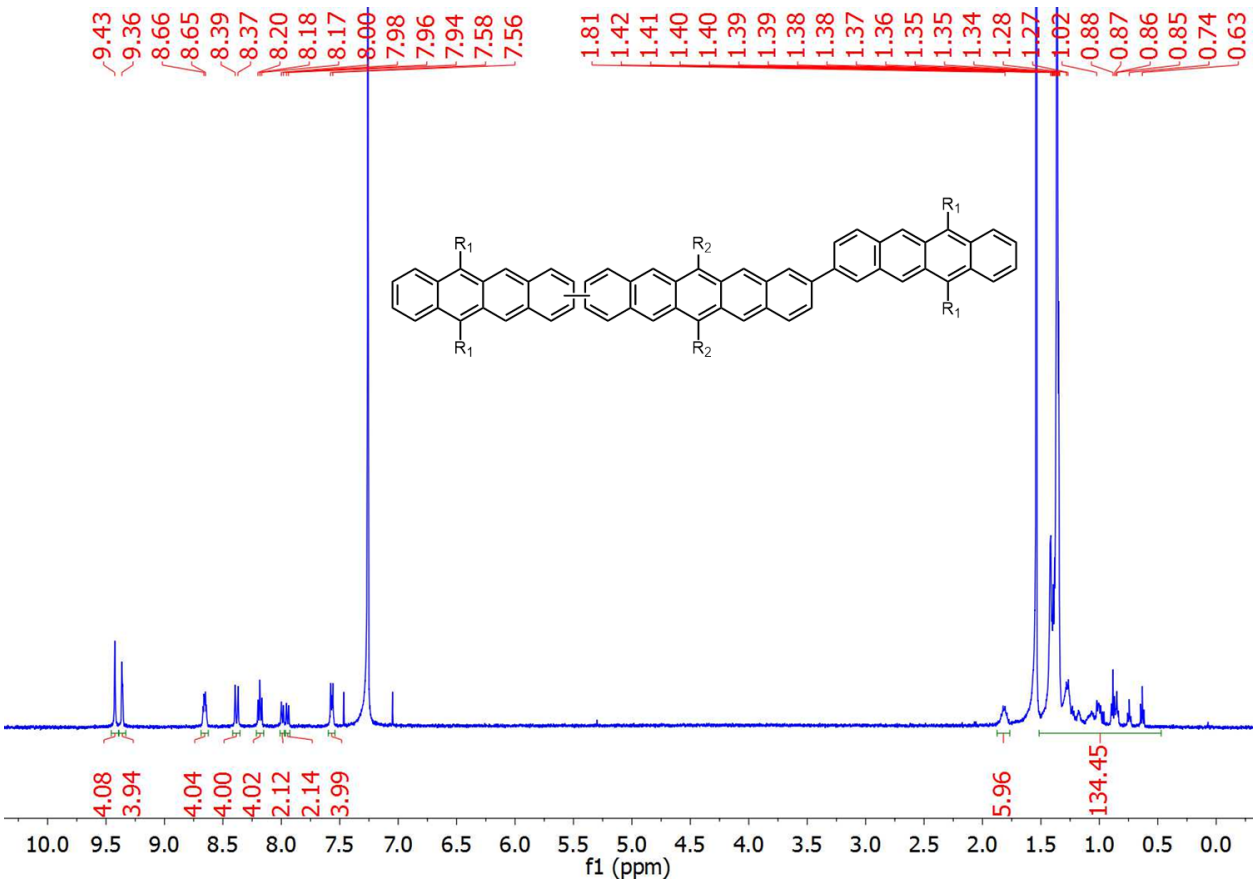
9.43
9.36
8.66
8.65
8.39
8.37
8.20
8.18
8.17
8.00
7.98
7.96
7.94
7.58
7.56
1.81
1.42
1.41
1.40
1.40
1.39
1.39
1.38
1.38
1.37
1.36
1.35
1.35
1.34
1.28
1.27
1.02
0.88
0.87
0.86
0.85
0.74
0.63
R1
R2
4.08
3.94
4.04
4.00
4.02
2.12
2.14
3.99
5.96
134.45
10.0 9.5 9.0 8.5 8.0 7.5 7.0 6.5 6.0 5.5 5.0 4.5 4.0 3.5 3.0 2.5 2.0 1.5 1.0 0.5 0.0
f1 (ppm)

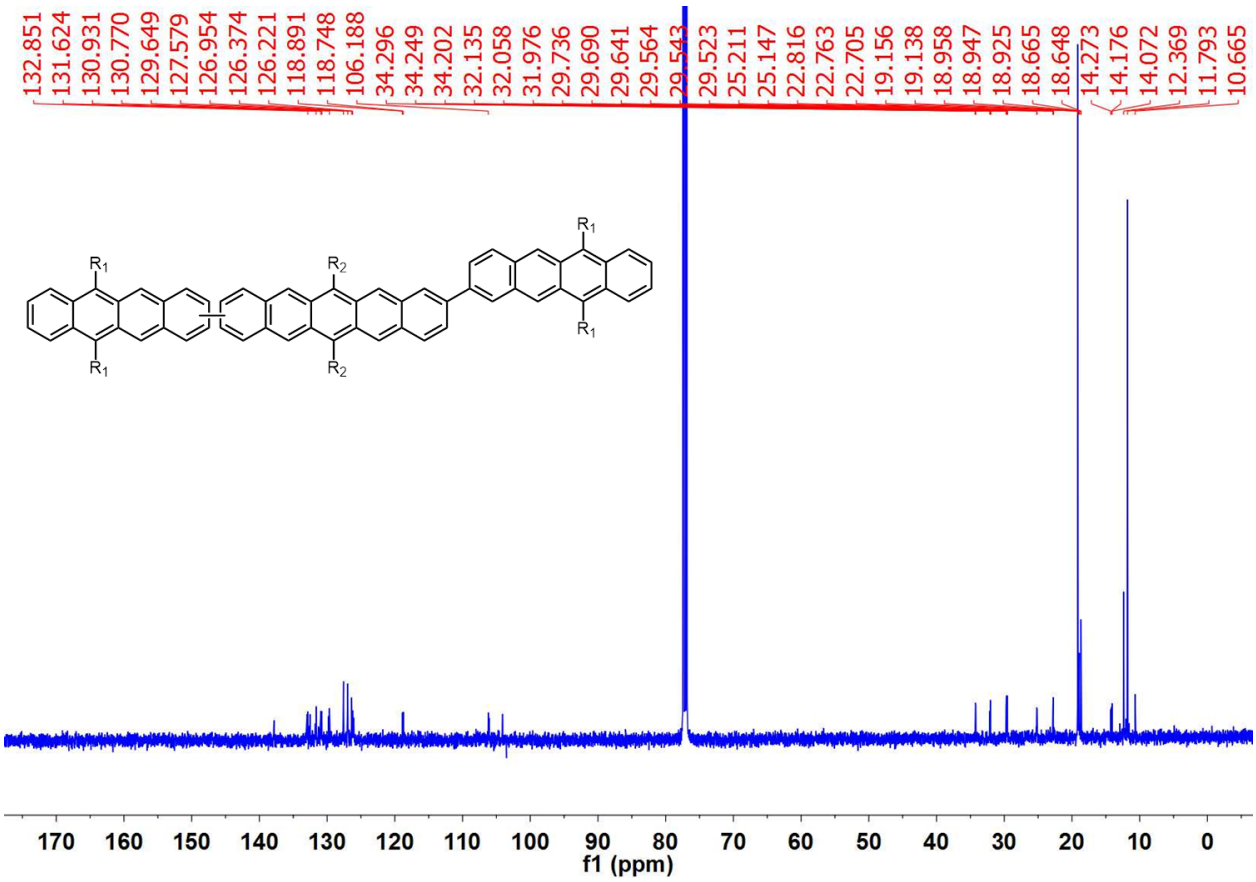
132.851
131.624
130.931
130.770
129.649
127.579
126.954
126.374
126.221
118.891
118.748
106.188
34.296
34.249
34.202
32.135
32.058
31.976
29.736
29.690
29.641
29.564
29.543
29.523
25.211
25.147
22.816
22.763
22.705
19.156
19.138
18.958
18.947
18.925
18.665
18.648
14.273
14.176
14.072
12.369
11.793
10.665
R1
R2
170 160 150 140 130 120 110 100 90 80 70 60 50 40 30 20 10 0
f1 (ppm)

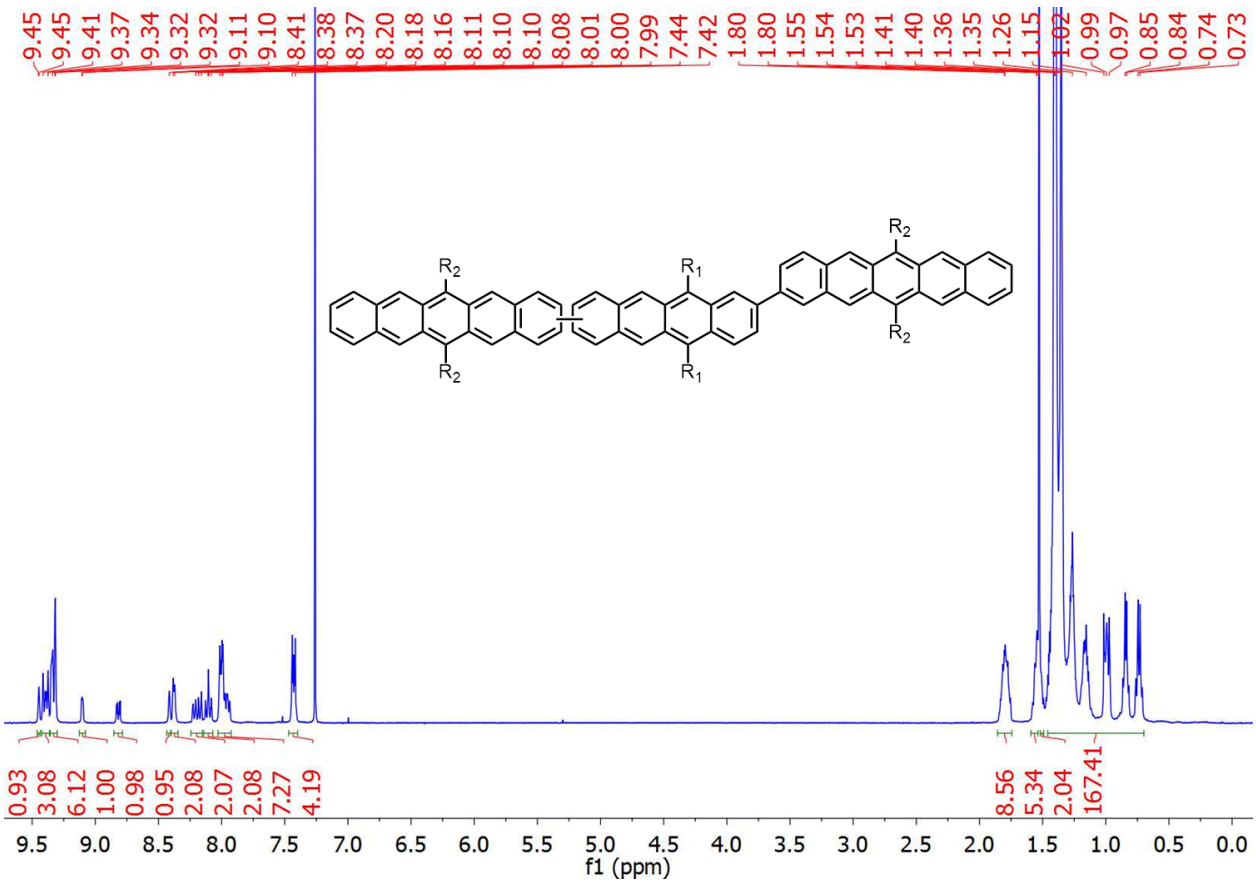
9.45
9.45
9.41
9.37
9.34
9.32
9.32
9.11
9.10
8.41
8.38
8.37
8.20
8.18
8.16
8.11
8.10
8.10
8.08
8.01
8.00
7.99
7.44
7.42
1.80
1.80
1.55
1.54
1.53
1.41
1.40
1.36
1.35
1.26
1.15
1.02
0.99
0.97
0.85
0.84
0.74
0.73
R2
R1
R2
R2
R1
R2
0.93
3.08
6.12
1.00
0.98
0.95
2.08
2.07
2.08
7.27
4.19
8.56
5.34
2.04
167.41
9.5
9.0
8.5
8.0
7.5
7.0
6.5
6.0
5.5
5.0
4.5
4.0
3.5
3.0
2.5
2.0
1.5
1.0
0.5
0.0
f1 (ppm)

.

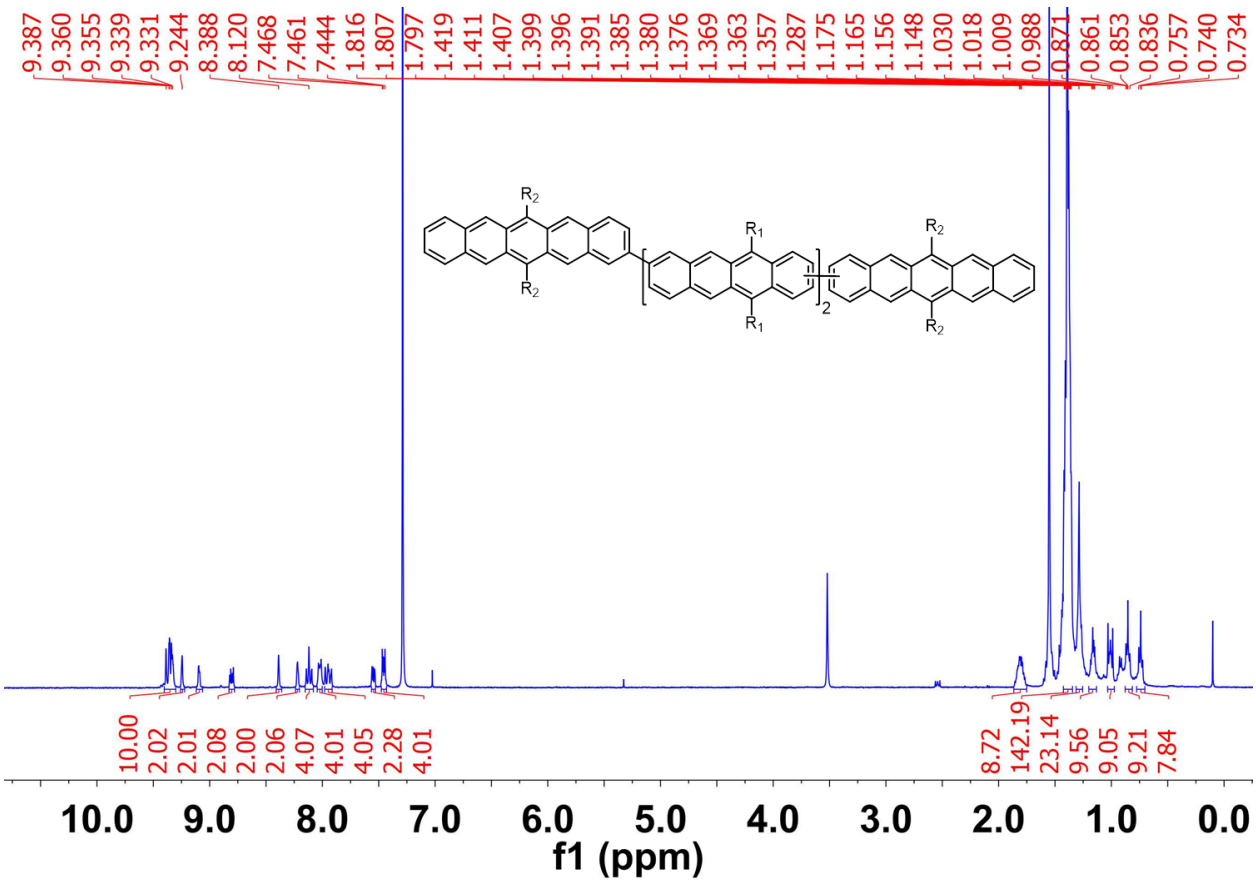
9.387
9.360
9.355
9.339
9.331
9.244
8.388
8.120
7.468
7.461
7.444
1.816
1.807
1.797
1.419
1.411
1.407
1.399
1.396
1.391
1.385
1.380
1.376
1.369
1.363
1.357
1.287
1.175
1.165
1.156
1.148
1.030
1.018
1.009
0.988
0.871
0.861
0.853
0.836
0.757
0.740
0.734
R2
R2
R1
R1
2
R2
R2
10.00
2.02
2.01
2.08
2.00
2.06
4.07
4.01
4.05
2.28
4.01
8.72
142.19
23.14
9.56
9.05
9.21
7.84
10.0
9.0
8.0
7.0
6.0
5.0
4.0
3.0
2.0
1.0
0.0
f1 (ppm)

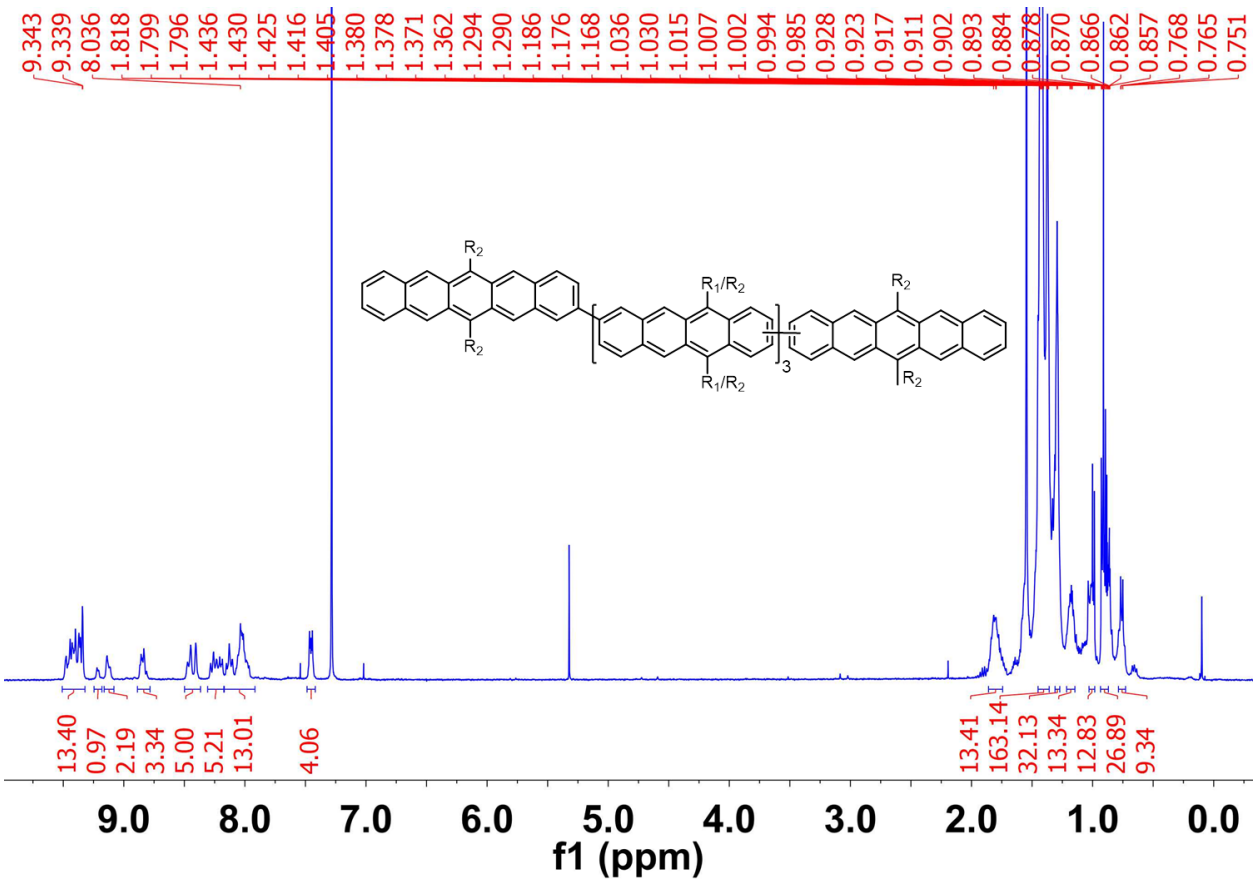
9.343
9.339
8.036
1.818
1.799
1.796
1.436
1.430
1.425
1.416
1.405
1.380
1.378
1.371
1.362
1.294
1.290
1.186
1.176
1.168
1.036
1.030
1.015
1.007
1.002
0.994
0.985
0.928
0.923
0.917
0.911
0.902
0.893
0.884
0.878
0.870
0.866
0.862
0.857
0.768
0.765
0.751
R2
R2
R1/R2
R1/R2
3
R2
R2
13.40
0.97
2.19
3.34
5.00
5.21
13.01
4.06
13.41
163.14
32.13
13.34
12.83
26.89
9.34
9.0
8.0
7.0
6.0
5.0
4.0
3.0
2.0
1.0
0.0
f1 (ppm)

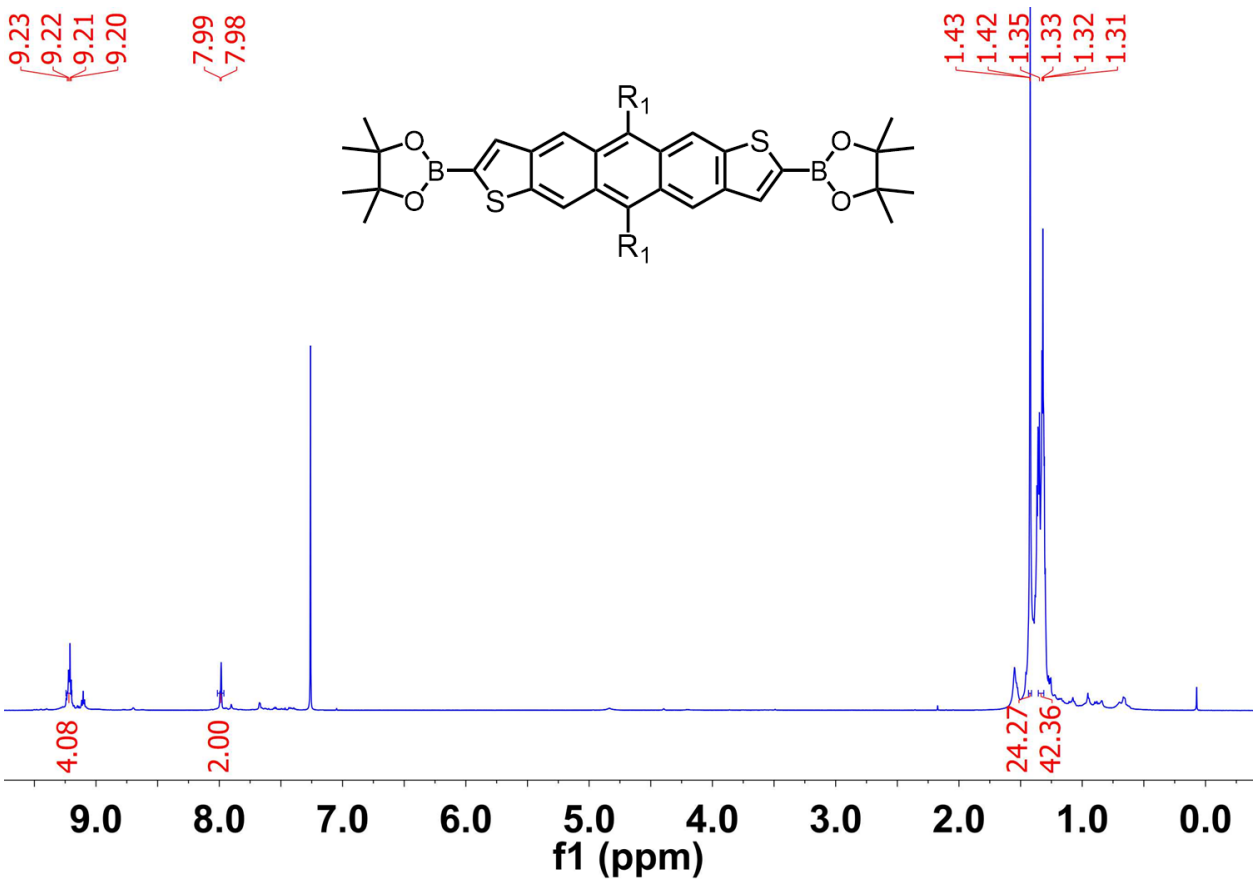
9.23
9.22
9.21
9.20
7.99
7.98
1.43
1.42
1.35
1.33
1.32
1.31
R1
R1
O
B
O
S
S
O
B
O
4.08
2.00
24.27
42.36
9.0
8.0
7.0
6.0
5.0
4.0
3.0
2.0
1.0
0.0
f1 (ppm)

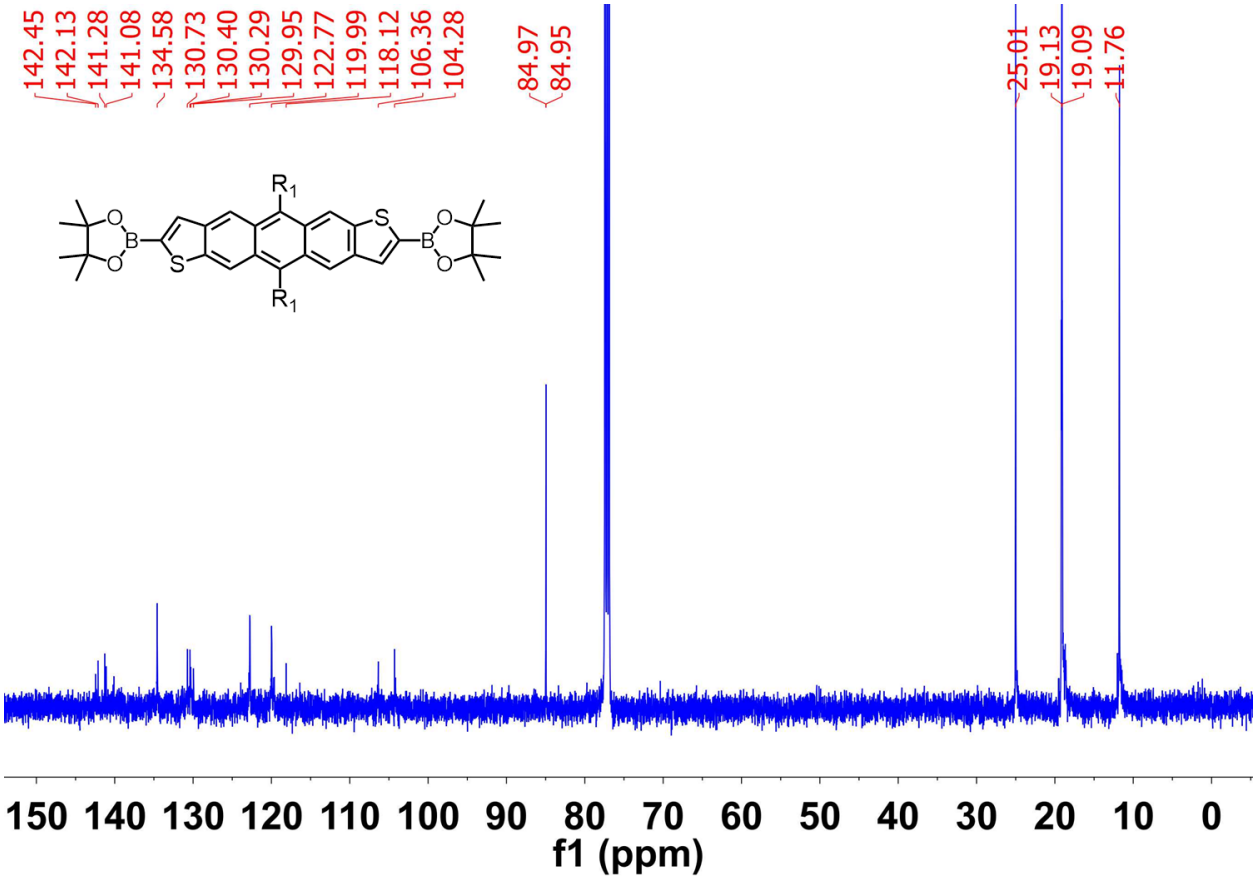
142.45
142.13
141.28
141.08
134.58
130.73
130.40
130.29
129.95
122.77
119.99
118.12
106.36
104.28
84.97
84.95
25.01
19.13
19.09
11.76
R1
R1
S
S
B
B
O
O
O
O
150 140 130 120 110 100 90 80 70 60 50 40 30 20 10 0
f1 (ppm)

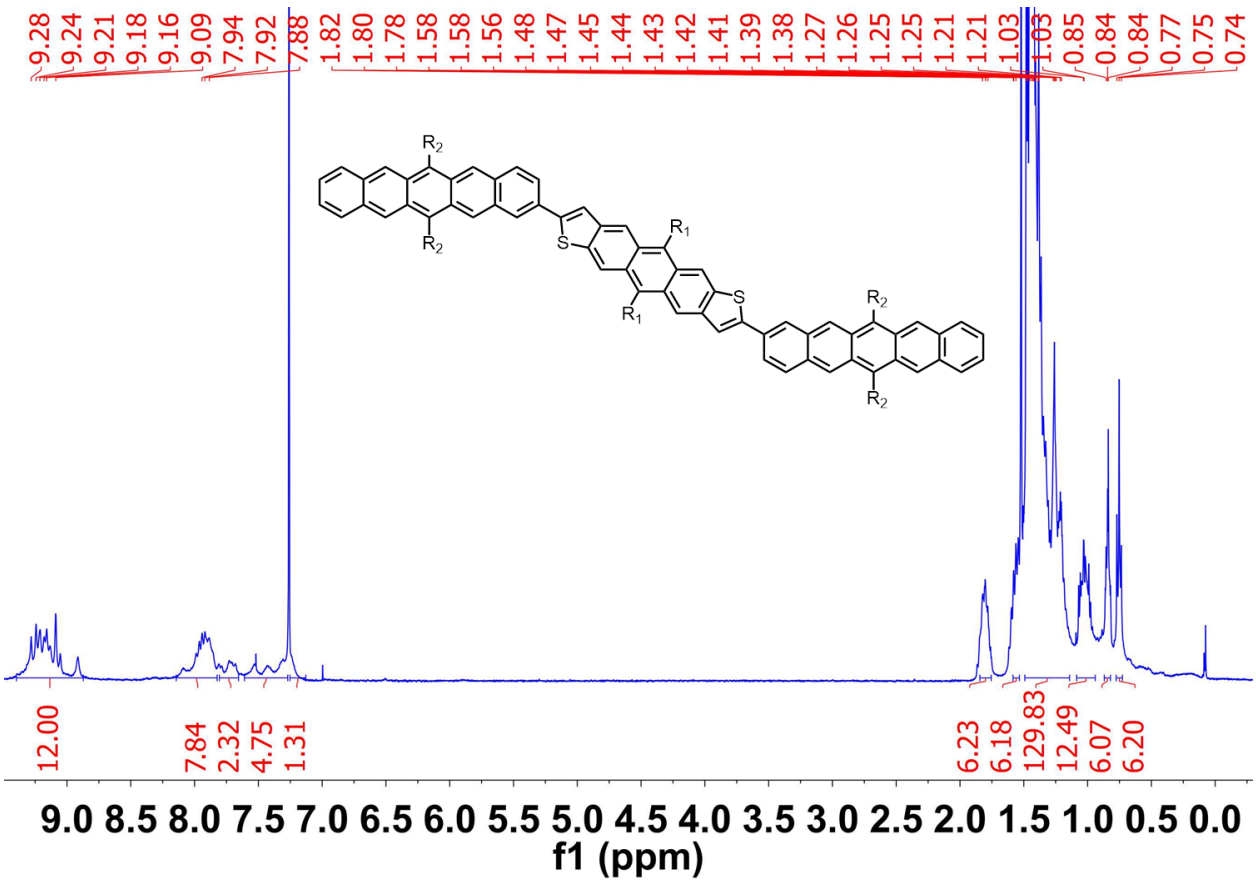
9.28 9.24 9.21 9.18 9.16 9.09 7.94 7.92 7.88 1.82 1.80 1.78 1.58 1.58 1.56 1.48 1.47 1.45 1.44 1.43 1.42 1.41 1.39 1.38 1.27 1.26 1.25 1.25 1.21 1.21 1.03 1.03 0.85 0.84 0.84 0.77 0.75 0.74
R2
R2
S
R1
R1
S
R2
R2
12.00 7.84 2.32 4.75 1.31 6.23 6.18 129.83 12.49 6.07 6.20
9.0 8.5 8.0 7.5 7.0 6.5 6.0 5.5 5.0 4.5 4.0 3.5 3.0 2.5 2.0 1.5 1.0 0.5 0.0
f1 (ppm)

13. References

1. Kumarasamy E, Sanders SN, Tayebjee MJY, Asadpoordarvish A, Hele TJH, Fuemmeler EG*, et al.* Tuning Singlet Fission in π-Bridge-π Chromophores. *Journal of the American Chemical Society*, **139**, 12488-12494 (2017).

2. Tayebjee MJY, Sanders SN, Kumarasamy E, Campos LM, Sfeir MY, McCamey DR. Quintet multiexciton dynamics in singlet fission. *Nat Phys*, **13**, 182-188 (2017).

3. Snellenburg JJL, S. P.; Seger, R.; Mullen, K. M.; van Stokum, I. H. M. Glotaran: A Java-Based Graphical User Interface for the R Package TIMP. *J Stat Soft*, **49**, 1-22 (2012).

4. Sanders SN, Kumarasamy E, Pun AB, Trinh MT, Choi B, Xia J*, et al.* Quantitative Intramolecular Singlet Fission in Bipentacenes. *Journal of the American Chemical Society*, **137**, 8965-8972 (2015).

5. Kazim S, Ramos FJ, Gao P, Nazeeruddin MK, Grätzel M, Ahmad S. A dopant free linear acene derivative as a hole transport material for perovskite pigmented solar cells. *Energy & Environmental Science*, **8**, 1816-1823 (2015).